Long-Rod Impact on Intact and Pre-Damaged Sleeved SiC Ceramics

Charles E. Anderson, Jr.[1]
Thilo Behner[2]
Dennis L. Orphal[3]
Timothy J. Holmquist[4]
Arthur E. Nicholls[1]

[1]Southwest Research Institute®
San Antonio, TX 78228

[2]Fraunhofer Institut fur Kurzzeitdynamik (Ernst-Mach-Insitut)
Freiburg, Germany

[3]International Research Associates, Inc.
Pleasanton, CA 94566

[4]Southwest Research Institute
Minneapolis, MN 55416

Contract: W56HZV-06-C-0194

SwRI® Report 18.12544/020

Prepared for:

US Army RDECOM-TARDEC
RDTA-RS
Warren, MI 43897-5000

July 2010

REPORT DOCUMENTATION PAGE

Form Approved
OMB No. 0704-0188

1. REPORT DATE *(DD-MM-YYYY)*	2. REPORT TYPE	3. DATES COVERED *(From - To)*
23/07/2010	Technical	Jan 2007 – Dec 2008

4. TITLE AND SUBTITLE

Long-Rod Impact on Intact and Pre-Damaged Sleeved SiC Ceramics

5a. CONTRACT NUMBER
W56HZV-06-C-0194

5b. GRANT NUMBER

5c. PROGRAM ELEMENT NUMBER

6. AUTHOR(S)

Charles E. Anderson, Jr.[1] and Thilo Behner[2], Dennis L. Orphal[3], Timothy J. Holmquist[4], and Arthur E. Nicholls[1]

5d. PROJECT NUMBER
18.12544

5e. TASK NUMBER

5f. WORK UNIT NUMBER

7. PERFORMING ORGANIZATION NAME(S) AND ADDRESS(ES)

[1]Southwest Research Institute, P.O. Drawer 28510, San Antonio, TX 78228-0510;
[2]Fraunhofer Institut fur Kurzzeitdynamik (Ernst-Mach-Insitut), Freiburg, Germany
[3]International Research Associates, Inc., Black Ave, Pleasanton, CA 94566
[4]Southwest Research Institute, 5353 Wayzata Blvd., Minneapolis, MN 55416

8. PERFORMING ORGANIZATION REPORT NUMBER

18.12544/020

9. SPONSORING/MONITORING AGENCY NAME(S) AND ADDRESS(ES)

US Army Tank-Automotive Research, Development, and Engineering Center, Warren, MI 48397-5000

10. SPONSOR/MONITOR'S ACRONYM(S)
TARDEC/RDTA-RS

11. SPONSORING/MONITORING AGENCY REPORT NUMBER

12. DISTRIBUTION AVAILABILITY STATEMENT

Approved for Public Release; Unlimited Distribution

13. SUPPLEMENTARY NOTES

The views, opinion, and/or findings contained in this report are those of the authors and should not be construed as an official Department of the Army position, policy, or decision, unless so designated by other documents.

14. ABSTRACT

Penetration experiments with long rods into SiC ceramics are available for two rod materials over a wide range of impact velocities [1-2]. The ceramics used in these experiments were initially intact, without cracks or other induced damage. The penetration response of three types of pre-damaged SiC was also investigated [3-4]. The pre-damaged targets, which were confined in 7075 aluminum sleeves consisted of 1) thermally shocked (many non-contiguous cracks), 2) thermally shocked with mechanical load/unload cycling (TS/CL or *in-situ* comminuted), and 3) compacted powder. This report describes additional experiments conducted on intact and thermally shocked (pre-damaged) SiC-N that overlapped the previous test data, and extend the data to lower impact velocities. It is found that the penetration velocity—within data scatter—is independent of whether the ceramic is initially intact or pre-damaged, which is a different result than expected.

15. SUBJECT TERMS

silicon carbide, penetration velocity, damage, ceramics, pre-damage

16. SECURITY CLASSIFICATION OF: Unclassified, Unlimited Distribution			17. LIMITATION OF ABSTRACT	18. NUMBER OF PAGES	19a. NAME OF RESPONSIBLE PERSON
					Mr. Rick Rickert
a. REPORT	b. ABSTRACT	c. THIS PAGE	None	60	19b. TELEPONE NUMBER *(Include area code)*
Unlimited	Unlimited	Unlimited			586-282-3194

Table of Contents

List of Figures

Page

List of Figures (Cont'd)

Page

List of Tables

Page

1.0 Introduction

Penetration experiments into silicon carbide (SiC) targets, over a wide range of impact velocities, have been conducted with tungsten [1] and gold [2] long rods. The experiments were conducted in the reverse ballistics mode; the cylindrical SiC "targets" were launched at long rods suspended in the flight path. Flash radiography was used to measure penetration depth versus time after impact. Gold was used in the second set of experiments to minimize the effect of penetrator strength. The penetration-time data are extremely linear; the slope of a linear regression of the penetration-time data gives the penetration velocity.

It has been very difficult to obtain independent laboratory measurements of the constitutive parameters for failed ceramics because they are so strong (e.g., loading platens fail before the confined specimen, confining sleeves yield and limit confining pressures, etc.). It was decided that a series of experiments to measure the penetration performance of a ceramic material with *initially* different strengths [3-4] would be of value for the study and development of computational ceramic constitutive models. Therefore, to assist in the determination of the strength of failed ceramic, ballistic experiments were performed on cylindrical SiC targets with three different grades or degrees of damage, described in the next section. These variously damaged ceramics, contained in an Al-sleeve, were launched in the reverse ballistic mode against stationary gold rods. Impact velocities ranged from 1 to 3 km/s.

This report is focused on the most recent experiments performed to extend the experimental database in Refs. [3-4] to lower impact velocities. Some of the impact velocities overlapped with the previous data so that direct comparisons could be made between the new and older data. After a review of the previous results, the new data will be summarized and compared to the older data.

2.0 Summary of Previous Results

The investigated ceramic was SiC-N from BAE Systems Advanced Ceramics Division—formerly Cercom—with a diameter of 18 mm and a length of 35 mm, placed inside (slip fit) a 7075-T6 aluminum sleeve of 31.5-mm outer diameter and a nominal 45-mm length (Fig. 1). The 7075-T6 base plate was machined with a 45-deg bevel, and then welded to the cylindrical sleeve. After the specimen was inserted into the Al sleeve, a 7075-T6 cover plate was press-fit into place using superglue. Three specimen types were prepared. 1) Thermally shocked (TS): pre-damage, in the form of non-contiguous cracks, was induced by 3 cycles of heating the specimen

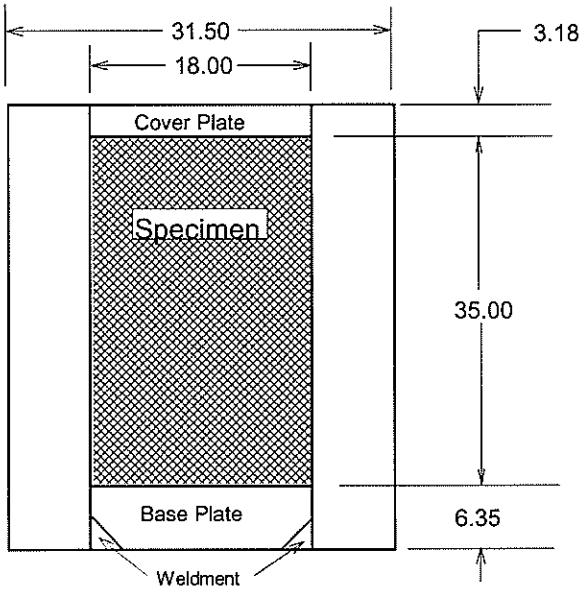

Figure 1. Test specimen with aluminum sleeve and cover plates (dimensions in mm).

for one hour at 750°C with a subsequent ice water quench; thereafter, placing in the Al-sleeve. Although cracked, the specimens have integrity and strength. 2) Thermally shocked/cyclic loaded (TS/CL or "*in-situ* comminuted"): specimens were thermally shocked as above and then subjected to six MTS machine loading/unloading cycles to 1.7 GPa while in the aluminum sleeve. After the cyclic loading, the loading anvils were removed and the cover and base plates were applied. The specimen, if removed from the aluminum sleeve, has interlocked comminuted pieces, and crumbles easily under a very small—"finger-pressure"—applied load. 3) Compacted powder (CP): SiC-N powder was placed into the Al-sleeve through a series of incremental pours and compaction using an MTS machine, achieving 72-73 % of the theoretical density of SiC-N ($\rho_{\text{comp. powder}} \approx 2.35$ g/cm^3). (Compacted powder is not a pre-damaged ceramic;

it is the raw material from which the intact SiC is fabricated. But for purposes of this report, we will use the word "damage" to describe all three specimen types.)

The experiments were conducted in the reverse ballistics mode, with the test specimen launched at a suspended gold rod with a diameter of 1.0 mm and length of 70 mm. Gold was used for the rod material to reduce the effect of rod strength while maintaining a high density. The penetration process was observed with five 180-kV flash X-rays. Since the gold rod erodes and generates a mushroom head, the foremost front of the gold in the ceramic was used as the penetration depth. Additional details on the experiments can be found in Ref. [3-4].

The position-time and rod length-time data are quite linear for most experiments. The thermally shocked targets were launched at high velocities (> 2.2 km/s); all of these had steady-state penetration. Steady-state penetration was observed for impact velocities above 1.8 km/s for the *in-situ* comminuted (TS/CL) ceramic, and above 1.5 km/s for the compacted powder specimens. The slope of the penetration-time regression gives the penetration velocity, u. The penetration velocities versus impact velocities for these previous experiments are shown in Fig. 2.

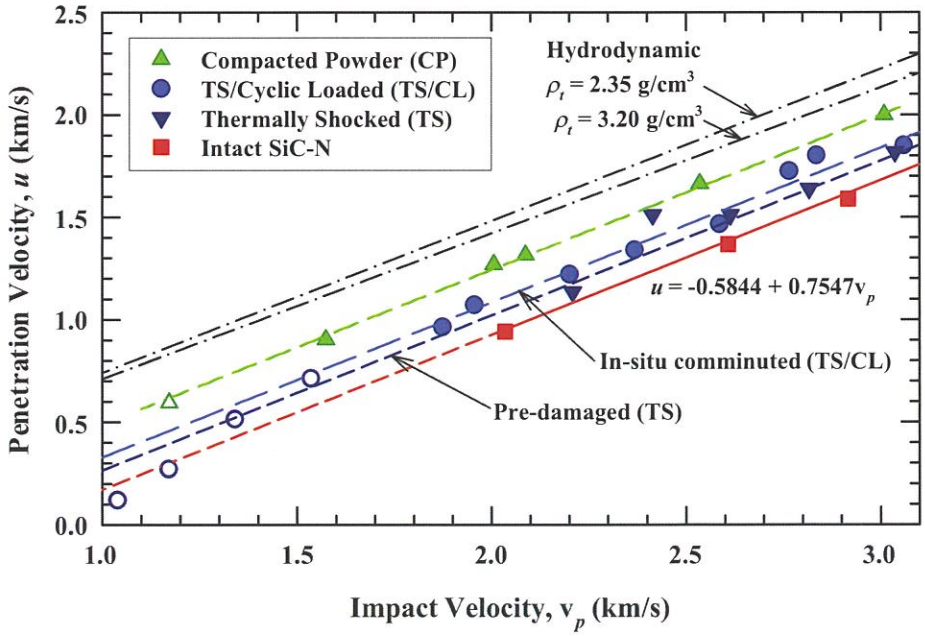

Figure 2. Penetration velocity u vs. impact velocity v_p for different types of SiC-N specimens.

Open symbols denote results where the penetration-time response was nonlinear over some or most of the penetration event. The penetration velocities of only the early or linear portion of penetration are plotted for these open symbols. Also included in the figure are the data for intact

(bare) SiC-N specimens from Ref. [2]. The data for the intact SiC extends to impact velocities of ~6 km/s; only the three lowest velocity data points are shown here.

The test series with intact SiC-N in [2] provided a linear relationship between penetration velocity u of the gold rod in the ceramic and impact velocity v_p:

$$u = -0.5844 + 0.7547 v_p. \quad (1)$$

For Eqn. (1), the velocities have units of km/s.

This regression line for intact SiC has been extrapolated in Fig. 2 to lower impact velocities, as indicated by the dashed line. We know that the u versus v_p response of intact SiC-N cannot be linearly extrapolated to the very low impact velocities shown in Fig. 2, because at some impact velocity the projectile begins to dwell at the target interface (for example, see [5-6]), but the linear extrapolation serves as a "trend" line.

The hydrodynamic lines are calculated from

$$u_{hydro} = \frac{v_p}{1 + \sqrt{\rho_t / \rho_p}} \quad (2)$$

where ρ_t and ρ_p are the target and projectile densities, respectively. The density for intact SiC-N is 3.20 g/cm^3, whereas the density for the compacted powder is 2.35 g/cm^3. The density of the Au rod is 19.3 g/cm^3.

Linear regression analyses were performed on the experimental data shown in Fig. 2, with the result that the slopes for TS, TS/CL, and CP were very similar to that for the intact SiC. Therefore, linear regression analyses were conducted to determine the intercepts for the TS, TS/CL, and CP data, *with the slope constrained to be 0.7547*, the value determined for the intact SiC data. These are the regression lines shown in Fig. 2. For the regression to the TS data, the data point at $v_p = 2.4$ km/s was omitted since it deviates more than 6.5 standard deviations from a regression fitted without the point. Examining Fig. 2, it is observed that:

$$u_{\text{intact}} < u_{\text{pre-damaged}} < u_{\text{in-situ comminuted}} < u_{\text{powder}} < u_{\text{hydrodynamic}} \quad (3)$$

corresponding to reductions in strength or resistance to penetration in the same order.

3.0 New Experimental Results

3.1 Introduction

A new experimental test series was developed with several objectives. First, we wanted to verify that the TS datum point at 2.4 km/s was really an outlier. Secondly, we wanted to extend the TS data to lower impact velocities. Next, intact SiC-N specimens were inserted into the aluminium sleeve to investigate if the presence of the sleeve affected penetration results (the experiments in Ref. [2] were done on bare SiC-N ceramic). A brief summary of the experimental procedures is provided, followed by a discussion of the essential results of these new experiments, including comparisons to the previous experiments.

3.2 Experimental Set-Up

The experimental arrangement was similar to that described above and documented in Refs. [3-4]. The ceramic was SiC-N ($\rho = 3.2$ g/cm^3) from BAE Systems Advanced Ceramics Division, with a diameter of 18 mm and a length of 35 mm. Two target sets were constructed:

- Six thermally shocked (TS) SiC-N specimens, denoted as TS-2, were prepared by heating for one hour at 750°C with a subsequent ice water quench (3 cycles), thereafter placing them in an Al-sleeve (Fig. 1);
- Six intact SiC-N specimens inserted into an Al sleeve (Fig. 1).

In all aspects, the target specimens and experimental procedures were the same as those described in Ref. [3-4], including the construction of the aluminum sleeve. The tests were performed with a two-stage light-gas gun, using a separating sabot to launch the ceramic targets (a non-separating sabot was used for the first few experiments but abandoned later due to large yaw). In order to achieve higher impact velocities, the outer diameter of the Al-sleeve was machined to 26 mm for $v_p > 2$ km/s to reduce the weight of the sabot. Results showed no influence from the reduced outer diameter.

The target packages were launched at a suspended gold (Au) rod. The rods were made of pure gold (99.99%) and had a diameter of 1.0 mm and a length of 70 mm. Material properties for the gold rod were: density $\rho_P = 19.3$ g/cm^3; hardness 65 HV5; UTS 220 MPa and elongation 30%. A laser was used to align the rod with the shotline.

The penetration process was observed with five 180-kV flash X-rays. Figure 3 shows the arrangement for the impact tank together with a position of the X-ray tubes for imaging the penetration process. The time measurements for the flash X-ray pictures are very accurate (to better than ±5 ns). Thus, measurement uncertainties lie in the accuracy of the position measurement from the flash X-ray pictures, which is about ± 0.1 to 0.15 mm.

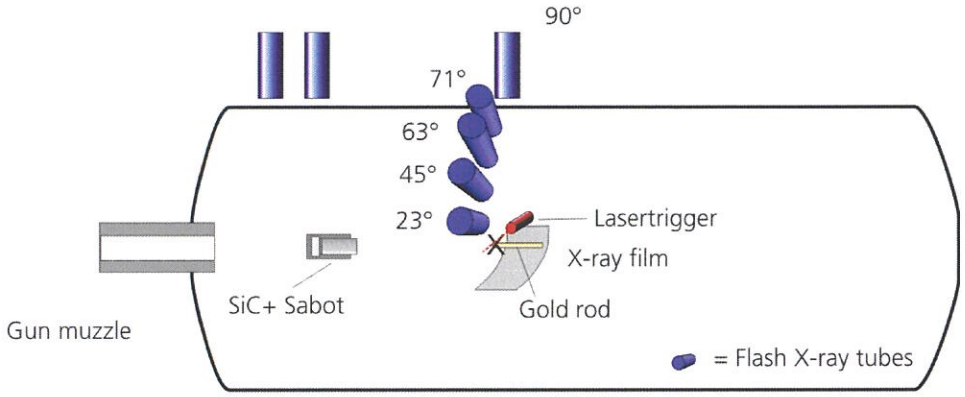

Figure 3. Blast tank with suspended gold rod and flash X-ray tubes.

3.3 Evaluation of Position-Time Data

An example of the flash X-ray data is shown in Fig. 4, Exp. 11346, which had an impact velocity, v_p, of 2.543 km/s. The trigger times for the X-rays are shown at the side of the figure. These trigger times are relative to impact on the cover plate. At each instance of time, the depth of penetration and the length of the rod were measured. The back (tail) of the rod does not move during the timeframe of the experiments (because the Au rod material has very low strength). The data for Exp. 11346 are plotted in Fig. 5. The ceramic surface is defined to be "0" in the spatial coordinates, thus impact occurs at -3.18 mm (the thickness of the cover plate).

The penetration-time and rod length-time data are linear (particularly at the higher impact velocities). Linear regression is applied to the data, but only for those data points that lie within the ceramic (since the rod has a different penetration rate while penetrating the cover plate). The linear regression results are shown in Fig. 5. The slopes of these curves are the penetration velocity and the rod consumption velocity, respectively; because the units are mm and μs, the rates are in mm/μs, or alternatively, km/s. For the example here, the penetration velocity u is 1.48 km/s, and the consumption velocity v_c is 1.09 km/s. (The consumption velocity is negative since the rod is getting shorter with time; however, for convenience, the consumption velocity is often reported as a positive quantity, as is done in this report.)

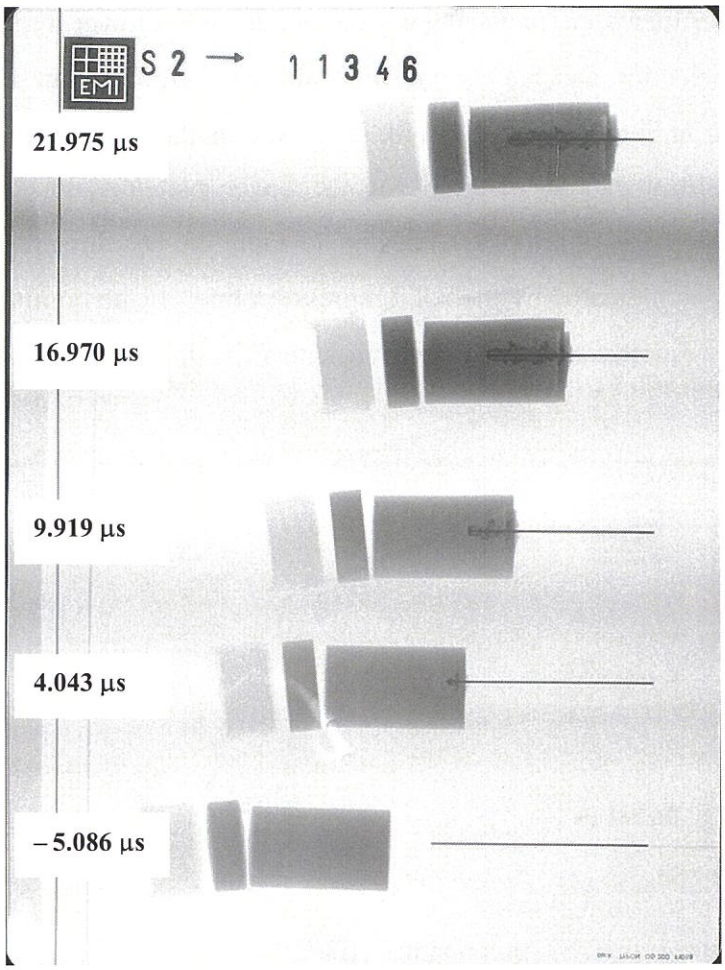

Figure 4. Example of flash X-ray images: Exp. 11346; v_p = 2.543 km/s.

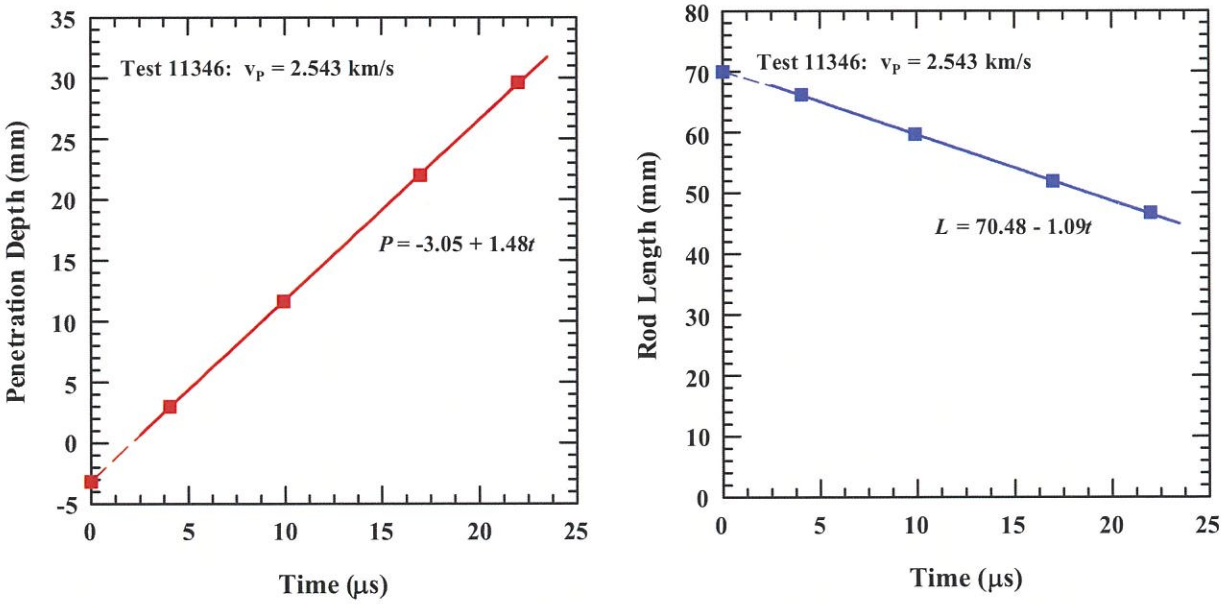

Figure 5. Penetration depth and rod length vs. time for Exp. 11346.

Some of the experiments, particularly the ones conducted at lower impact velocities, exhibit dwell or dwell-like behavior, and the early portion of the penetration-time response is nonlinear. An example is shown in Fig. 6 for Exp. 11340. The callouts denote that the rod has dwelled—as indicated by radial flow of rod material—at the cover plate/ceramic interface. The data measured from the flash X-rays are plotted in Fig. 7. Only the last three data points are used for the linear regression, as indicated by the solid regression line. If the nominally linear portion of the penetration-time response is extrapolated back to $P = 0$, then the estimated dwell time is 9.4 μs.

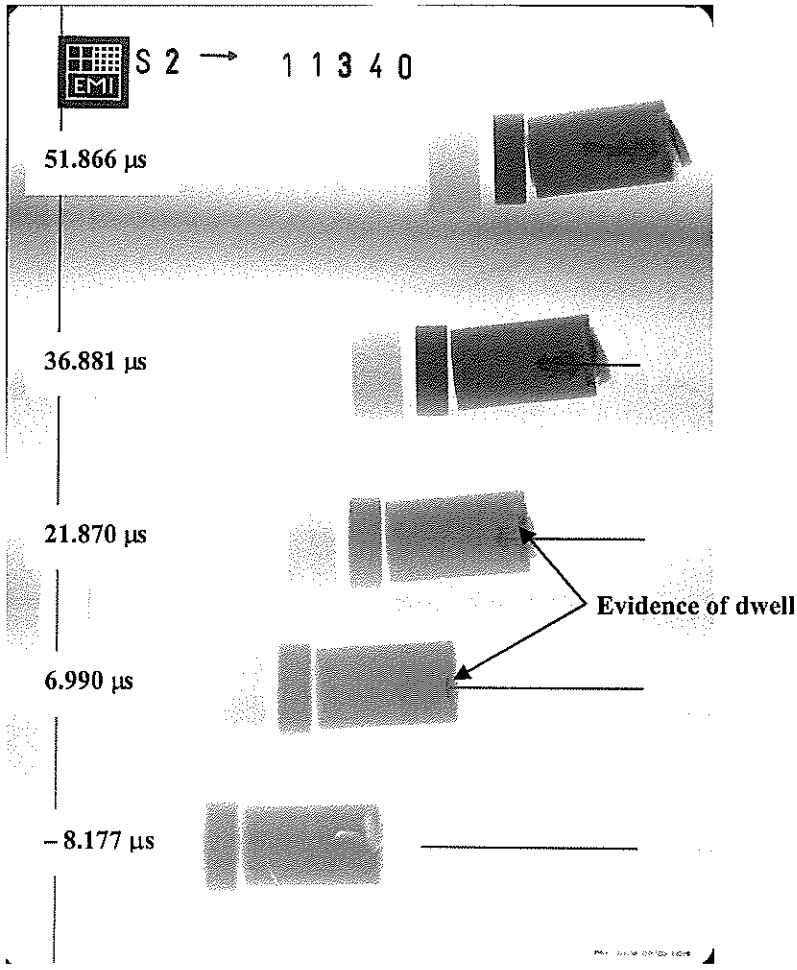

Figure 6. Flash X-ray for Exp. 11340 showing evidence of dwell; $v_p = 1.497$ km/s.

The flash X-rays and graphical representation of all 12 experiments are provided in the Appendix. The experimentally measured penetration depths and rod lengths, as a function of time after impact, are listed in Table A-1 by test number. The penetration velocity and consumption velocity for each experiment, u and v_c, respectively, were calculated from linear regression of the data as described for Figs. 5 and 7. The solid lines readily identify which data

were used for conducting the regression analysis. The results, sorted by increasing impact velocity, v_p, are summarized in Table 1.

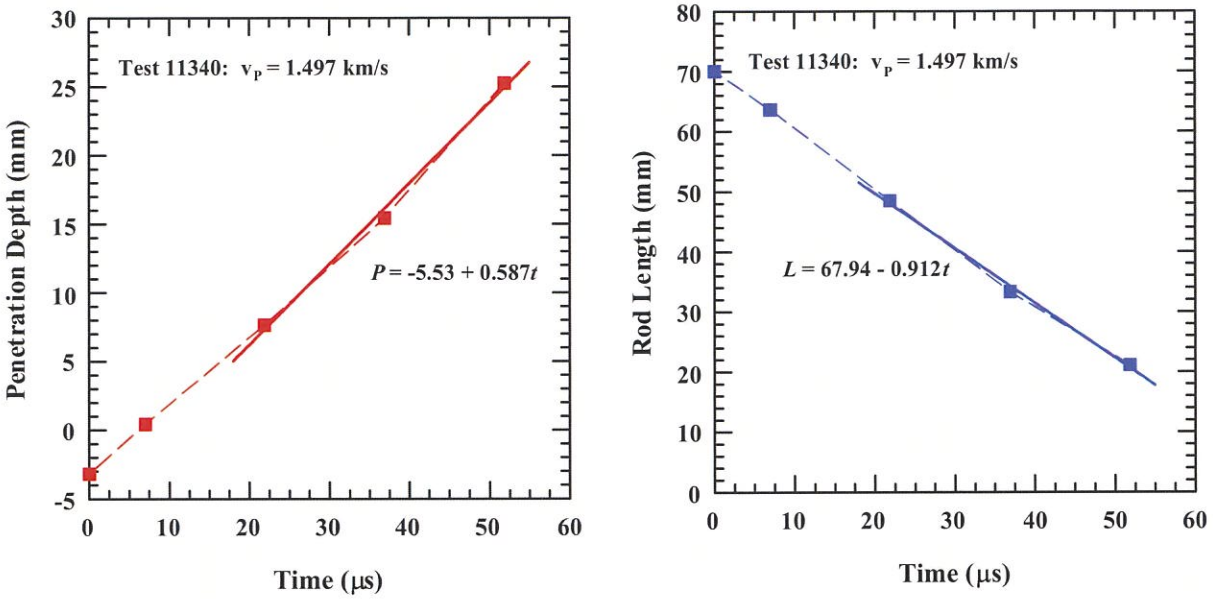

Figure 7. Penetration depth and rod length vs. time for Exp. 11340.

Table 1. Experimental Results

Exp	Target	yaw [°]	oc [mm]	v_p [km/s]	u [km/s]	v_c [km/s]
11349	TS13	2.2	2.1	1.248±0.005	0.332±0.034	0.941±0.034
11351	TS14	0.7	1.5	1.280±0.005	0.533±0.008	0.734±0.007
11341	TS9	1.5	0.8	1.517±0.004	0.737±0.024	0.786±0.023
11343	TS10	4.3	3.5	2.122±0.008	1.222±0.021	0.903±0.022
11345	TS11	3.1	2.1	2.358±0.011	1.344±0.011	1.002±0.037
11346	TS12	3.1	2.3	2.543±0.013	1.482±0.008	1.087±0.010
11350	IT6	7.1	3.0	1.234±0.006	0.115±0.010	1.142±0.013
11340	IT1	7.5	2.3	1.497±0.006	0.587±0.039	0.912±0.057
11342	IT2	5.9	3.2	2.170±0.008	1.149±0.058	1.028±0.053
11348	IT5	1.6	1.4	2.511±0.004	1.424±0.004	1.076±0.015
11344	IT3	2.0	0.0	2.564±0.008	1.533±0.028	1.043±0.020
11347	IT4	1.6	1.5	3.051±0.017	1.881±0.039	1.187±0.058

3.4 Comparison of New Data to Previous Data

3.4.1 New Thermally Shocked (TS-2) Ceramic Data

The first objective was to verify whether the TS datum point at 2.4 km/s was really an outlier, and then the TS data were extended to lower impact velocities. Six TS SiC-N targets (denoted as TS-2) were prepared as described above. Impact velocities were varied between 1.248 and 2.543 km/s. The results are shown as the inverted open triangles in Fig. 8. Several observations can readily be made. The new data between approximately 2.1 km/s and 2.5 km/s shows that the original TS datum point at 2.4 km/s does, indeed, have a higher penetration velocity than the new data. However, no longer do all the TS data lie consistently below the *in-situ* comminuted results (the solid circles). In fact, within data scatter, there appears to be no difference in the penetration response of the two types of damaged (TS and TS/CL) SiC-N.

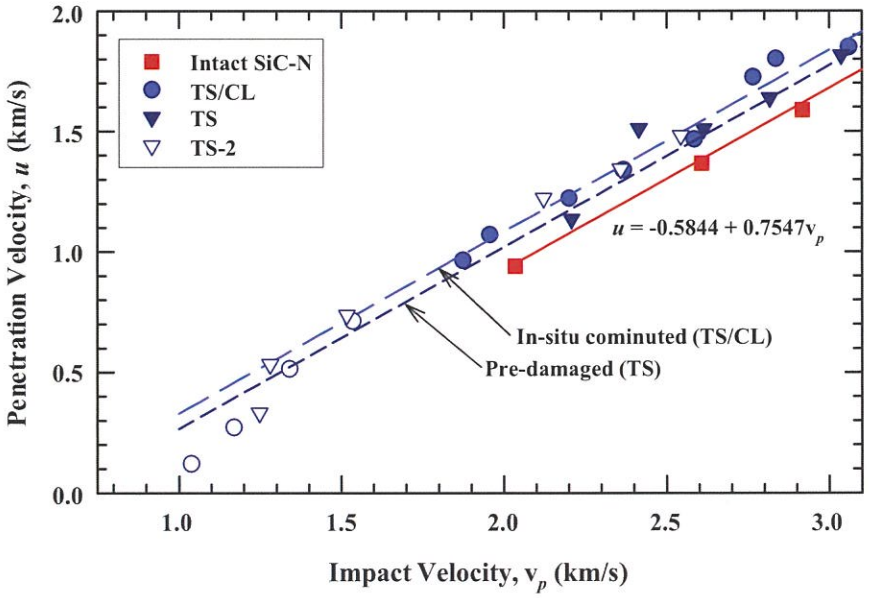

Figure 8. Comparison of new thermally shocked specimens (TS-2) with previous experimental results.

At impact velocities less than ~1.5 km/s, some portion of the penetration is nonlinear in time. For the new TS-2 data, only the nominally linear penetration-time data were used to estimate the penetration velocity, similar to what was done previously for the lower velocity

TS/CL results (open circles)[1]. At the lower impact velocities, the new TS-2 data are also indistinguishable from the TS/CL results with respect to penetration response.

3.4.2 Sleeved Intact Ceramic Data

Next, six intact SiC-N specimens were tested (18-mm diameter, 35-mm long, inserted in the Al sleeve). These experiments differed from the original intact series, which were done with 20-mm diameter and 35-mm long, bare (no sleeve or cover plate) SiC-N cylinders. The objective for these new experiments was to investigate if the aluminum confinement influenced penetration results. One other difference is that the original intact experiments [2] were conducted with 0.75-mm diameter, 50-mm-long Au rods; whereas, all the more recent experiments were conducted with 1.00-mm diameter, 70-mm long Au rods. (The larger diameter rod was adopted to facilitate handling and positioning of the Au rods in the target chamber.)

Previous work had demonstrated that the diameter of the target should have no effect at higher impact velocities [7]; however, numerical simulations indicate that penetration velocity increases at lower impact velocities, e.g., ~1.2 – 1.5 km/s, for these targets. Therefore, the test series was designed to obtain data over a velocity range of approximately 1.2 to 3.0 km/s. The results are shown in Fig. 9 as the solid hexagons. It was expected that the presence of the cover plate would affect the lowest velocity experiment by allowing dwell [6], and the lowest impact velocity of 1.234 km/s showed dwell-like behavior and very little penetration. However, the results at the higher impact velocities were clearly surprising. *The penetration response of these intact (but confined within the aluminum cylinder) SiC-N cylinders cannot be distinguished from the penetration response of the two pre-damaged SiC-N specimens (circles and inverted triangles).*

The SiC-N specimens for these new experiments come from a different production lot than the older experiments (two purchase orders separated by several years). However, each lot had standard characterization tests conducted and reported (density, longitudinal and shear sound velocities, Poisson's ratio, Young's modulus, shear modulus, and Knoop hardness), and the results for the two lots agree within measurement accuracies. Further, our experience is that the

[1] Previously, a distinction was made between penetration-time (*P-t*) data that were linear (solid symbols) versus a response that was nonlinear (open symbols) over some portion of the *P-t* data set. This distinction has been dropped as we examine the new experimental data. The reader can examine the graphs in the Appendix to assess the linearity of the new data.

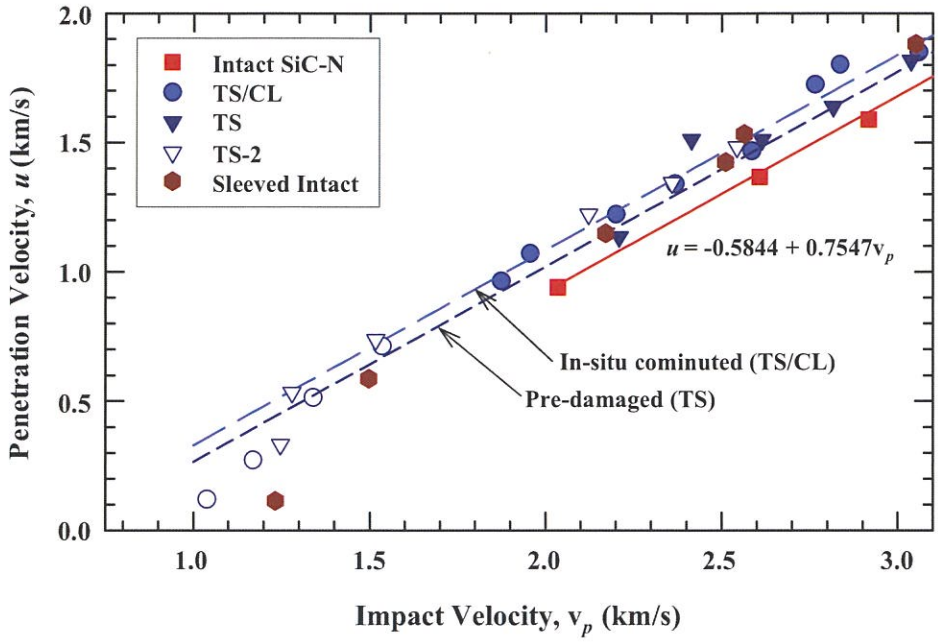

Figure 9. Comparison of new intact sleeve experiments with previous experiments.

processing and fabrication of SiC-N specimens by BAE Systems Advanced Ceramics, Inc., is highly controlled. Thus, we do not believe the difference in the penetration response between the new and old intact experiments is due to differences in the two lots of SiC-N.

3.4.3 New Intact, Bare Ceramic Data

A test series was also designed to investigate interface defeat and the transition from dwell to penetration [8-10]. There were eight experiments for bare, 20-mm-diameter SiC-N targets (no aluminum sleeve was used for these experiments). The Au rods were all 1.00-mm in diameter. Because the interest was in dwell and interface defeat, the impact velocities were relatively low, all below ~1.6 km/s. The open squares in Fig. 10 denote the penetration velocities as a function of impact velocity for these eight experiments. Interface defeat on a bare ceramic was observed at an impact velocity of 0.776 km/s. Otherwise, the penetration response is similar to the other 1.00-mm-diameter Au rod data. As these experiments did not have the aluminum sleeve or cover plate, and since there is no difference in the penetration response of the intact and pre-damaged targets, it is unlikely that the disagreement between the original intact data [2] and these newer data can be explained by differences in confinement.

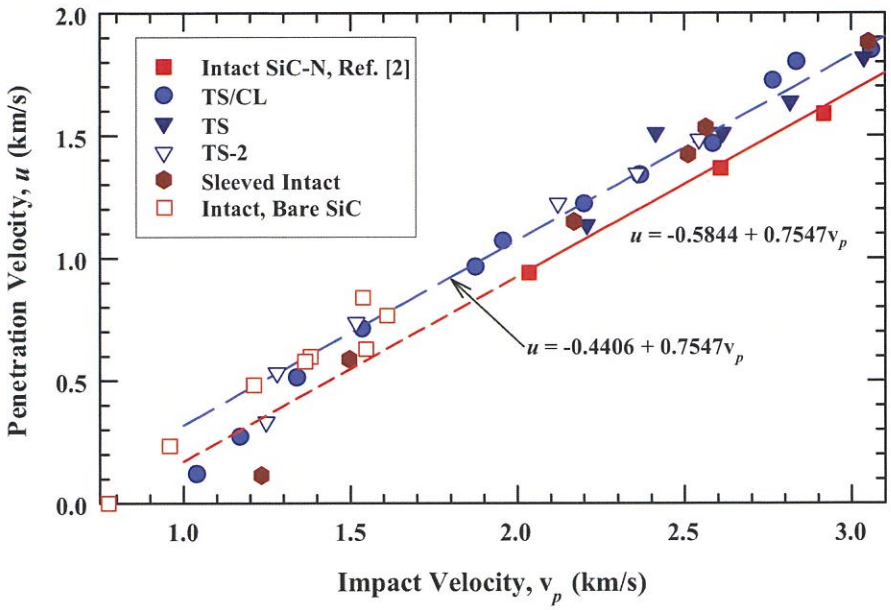

Figure 10. Comparison of intact, bare low-velocity results with new and previous experiments.

3.4.4 Updated Penetration Velocity vs. Impact Velocity Relationship

Within data scatter, there is no difference in the penetration velocity as a function of impact velocity for the new bare intact, sleeved intact, thermally shocked pre-damaged (TS and TS-2), and thermally shocked with cyclic loading (TS/CL) predamaged silicon carbide. A linear regression analysis was conducted on all the TS/CL, TS, TS-2, sleeved intact, and the new intact bare data (open squares in Fig. 10) with a penetration velocity greater than 0.40 km/s. Deleting the data with a penetration velocity less than 0.40 km/s eliminated the obvious nonlinear penetration response data. This removed 6 of the data points, leaving a total of 31 data points in the regression set. The "outlier" at 2.4 km/s *was* included in the data set, as it appears, when combining all these data, that this point does not deviate from the average significantly more than several other points. The slope of the linear fit was fixed at 0.7547 as was done previously (the slope on the original intact SiC-N data was determined over a velocity range of 2.0 – 6.0 km/s). With this constrained slope, the regression analysis of the 31 data points gives:

$$u = -0.4406 + 0.7547v_p. \quad (4)$$

with an r^2 value of 0.985. The standard deviation for the fit on penetration velocity is 56.9 m/s. Conducting a two-parameter regression analysis (to determine the slope as well as the intercept) only changes the slope by 1.7%, with essentially no improvement in the regression statistics.

Equation (4) is plotted as the long dashed line in Fig. 10. As was done in Fig. 2, the solid line is extrapolated to lower impact velocities in Fig. 10, denoted by the short dashed line. It is

observed that all "new" data (all data except the original Ref. [2] data) lie above the extrapolated and solid lines for the original intact SiC data (solid squares in Fig. 10), although there are a couple of new data points at ~1.5 km/s that are near the extrapolated line (as well as one TS datum at ~2.2 km/s).

3.4.5 Post-Dwell Penetration Data

Eight reverse ballistic experiments were conducted with a thin copper buffer (4 mm) or copper plate (2 mm) on otherwise unconfined SiC-N targets (20-mm diameter). The copper buffer/plate diminishes the effect of the impact shock, and provides ramp loading to the underlying ceramic [6, 10]. Additional details regarding the design of these experiments are given in Ref. [9]. The data are plotted as the solid triangles in Fig. 11. With this Cu buffer, complete interface defeat was observed at an impact velocity of 1.382 km/s. At slightly higher impact velocities, the projectile dwells, and then transitions to penetration. It has been seen experimentally, by comparing the results of Lundberg, *et al.* [11] to those of Orphal and Franzen [1], and that of our own data [8-10] that the penetration velocity after dwell is, within data scatter, the same as if no dwell had occurred. These post-dwell penetration velocities (the solid triangles in Fig. 11) are consistent with the non-dwell penetration velocity data.

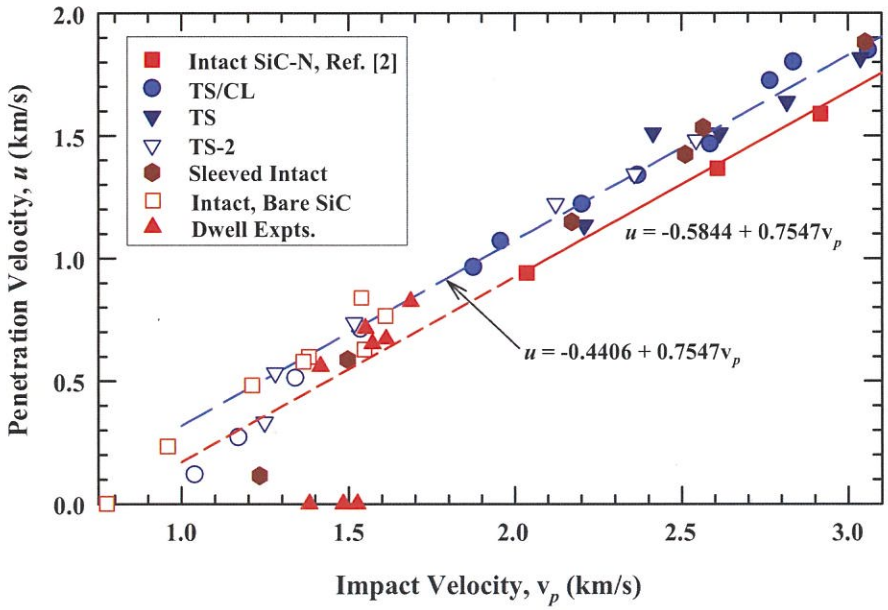

Figure 11. Results of dwell experiments after transition from dwell to penetration.

3.4.6 Summary

Comparing the results of Figs. 10 or 11 with those of Fig. 2, we rewrite Eqn. (3) as:

$$u_{\text{intact}} \approx u_{\text{pre-damaged}} \approx u_{\text{in-situ comminuted}} < u_{\text{powder}} < u_{\text{hydrodynamic}} \quad (5)$$

A natural question is: Why is there no difference in the penetration response of intact and damaged ceramic (above the dwell transition velocity)? A possible answer is that once damage is initiated, a damage front propagates into the ceramic, and propagates faster than the penetration velocity. This has been observed for lead glass and borosilicate glass [12-13]. Because glass is transparent, damage can be visualized optically. Flash radiography was also used, so that there could be a direct comparison of the leading edge of damaged glass and the rod penetration front. It was found, except for the initial transition of intact to damaged glass, that the projectile was penetrating damaged glass. This may be a characteristic behavior of very brittle materials.

We make one last observation. It appears that the penetration response, as measured by u, of pre-damaged ceramic and that of intact ceramic at low impact velocities, has more variability than that of intact ceramic at higher impact velocities. In particular, note the scatter in the data represented by the open squares and solid triangles (not including sustained dwell) between 1.5 and 1.6 km/s; although the highest u (open square) had one of the worst off-centered impacts combined with high yaw. The caution, then, is that one can be mislead by examining only one datum. Rather, it is an average penetration response that needs to be considered in evaluating the penetration resistance of a ceramic.

4.0 Conclusions

The new experimental data lead to two surprising results: 1) the ballistic resistance of the intact targets from Ref. [2] is larger (slower penetration velocity) than for the intact targets presented here; and 2) the new data indicate that there is no significant difference in the penetration response of intact (bare or sleeved) ceramic versus pre-damaged (thermally shocked or *in-situ* comminuted, i.e., TS, TS-2, and TS/CL) ceramic, which is different than the results reported in Ref. [3-4] (which concluded, from a smaller experimental data set, that penetration resistance decreased with increasing damage to the ceramic). In analogy to glass, it is reasoned that a damage front propagates faster than the penetration front [12-13]; and therefore, the projectile penetrates damaged (highly comminuted) material. This idea was first proposed in computational modeling of tungsten-alloy long rods into glass [14], prior to any experimental evidence. This concept—assuming that the projectile penetrates failed ceramic—was carried further by Walker when he showed good agreement between an analytic model and penetration of thick ceramic by long rods [15-16].

But then, why the discrepancy between the penetration velocities of the initial experiments of Ref. [2] and the results presented here? One difference is that the intact experiments of Ref. [2] used a 0.75-mm diameter Au rod, and the intact experiments reported here had a diameter of 1.0 mm. Recently, Andersson, *et al.* [17], suggested a projectile size effect for the dwell transition velocity, but made no predictions concerning the penetration velocity. Therefore, to provide insight into these surprising results, additional experiments are planned using 20-mm-diameter SiC-N cylinders (from the same production lot). No aluminum confinement will be used. The cylinders will be launched at suspended Au rods 0.75 mm and 1.0 mm in diameter, over a velocity range of 2.2 to 3.0 km/s. The results of these planned experiments seem sure to be informative.

5.0 Acknowledgements

The authors would like to thank Dr. Douglas Templeton and Mr. Rick Rickert of RDECOM-TACOM for their technical, administrative and financial support of this research effort. We also thank Ms. Nikki King (SwRI) for her assistance in plotting the experimental data and re-checking the results of the regression analyses.

6.0 References

1. D. L. Orphal and R. R. Franzen, "Penetration of confined silicon carbide targets by tungsten long rods at impact velocities from 1.5 to 4.6 km/s," *Int. J. Impact Engng.*, **19**(1): 1-13 (1997).
2. T. Behner, D. L. Orphal, V. Hohler, C. E. Anderson, Jr., R. L. Mason, and D. W. Templeton, "Hypervelocity penetration of gold rods into SiC-N for impact velocities from 2.0 to 6.2 km/s," *Int. J. Impact Engng.*, **33**(1-12): 68-79 (2006).
3. C. E. Anderson, Jr., T. Behner, D. L. Orphal, A. E. Nicholls, V. Hohler, and M. Wickert, "Time-resolved penetration into pre-damaged, in-situ comminuted, and compacted powder silicon carbide," SwRI Report 18.12544/001, prepared for U. S. Army RDECOM-TARDEC, AMSRD-TAR-R, Warren, MI, October (2007).
4. C. E. Anderson, Jr., T. Behner, D. L. Orphal, A. E. Nicholls, and D. W. Templeton, "Time-resolved penetration into pre-damaged hot-pressed silicon carbide," *Int. J. Impact Engng.*, **35**(8): 661-673 (2008).
5. T. J. Holmquist and G. R. Johnson, "A detailed computational analysis of interface defeat, dwell and penetration for a variety of ceramic targets," *Proc. 20th Int. Symp.Ballistics*, **2**: 746-753, DES*tech* Publications, Inc., Lancaster, PA (2002).
6. T. J. Holmquist, C. E. Anderson, Jr., and T. Behner, "Design, analysis and testing of an unconfined ceramic target to induce dwell," *Proc. 22th Int. Symp. Ballistics*, **2**: 860-868, DES*tech* Publications, Inc., Lancaster, PA (2005).
7. I. S. Chocron, C. E. Anderson, Jr., T. Behner, and V. Hohler, "Lateral confinement effects in long-rod penetration of ceramics at hypervelocity," *Int. J. Impact Engng.*, **33**(1-12): 169-179 (2006).
8. T. Behner, C. E. Anderson, Jr., T. J. Holmquist, M. Wickert, and D. W. Templeton, "Interface defeat for unconfined SiC ceramics," *Proc. 24th Int. Symp. Ballistics*, **1**: 35-42, DES*tech* Publications, Inc., Lancaster, PA (2008).
9. C. E. Anderson, Jr., T. Behner, T. J. Holmquist, D. L. Orphal, and M. Wickert, "Dwell, interface defeat, and penetration of long rods impacting silicon carbide," SwRI Report 18.1244/008, prepared for RDECOM-TARDEC, AMSRD-TAR-R, Warren, MI, November (2009).
10. T. J. Holmquist, C. E. Anderson, Jr., T. Behner, and D. L. Orphal, "The mechanics of dwell and post-dwell penetration," *Advances in Applied Ceramics*, **109**(8): xxx-xxx (2010).
11. P. Lundberg, R. Renstrom, and B. Lundberg, "Impact of metallic projectiles on ceramic targets: transition between interface defeat and penetration," *Int. J. Impact Engng.*, **24**(3): 259-275 (2000).
12. T. Behner, C. E. Anderson, Jr., D. L. Orphal, V. Hohler, M. Moll, and D. W. Templeton, "Penetration and failure of lead and borosilicate glass against rod impact," *Int. J. Impact Engng.*, **35**(6): 447-456 (2008).
13. D. L. Orphal, "Some recent results on the propagation of the failure front associated with rod penetration of borosilicate glass," ***Shock Compression of Condensed Matter – 2009*** (M. L. Elert, et al., Eds.), AIP Conf. Proc. 1195: 1425-1430, AIP Press, Melville, NY (2009).
14. C. E. Anderson, Jr., V. Hohler, J. D. Walker, and A. J. Stilp, "Modeling long-rod penetration into glass targets," *14th U. S. Army Symp. on Solid Mech.*, (K. R Iyer and S-C Chou, Eds.), pp. 129-136, Battelle Press, Columbus, OH (1996).
15. J. D. Walker, "Analytic model for penetration of thick ceramic targets," ***Ceramic Armor Materials by Design*** (J. W. McCauley, et al, Eds.), *Ceramic Transactions*, **134**: 337-348 (2002).

16. J. D. Walker, "Analytically modeling hypervelocity penetration of thick ceramic targets," *Int. J. Impact Engng.*, **29**(1-12): 747-755 (2003).

17. O. Andersson, P. Lundberg, and R. Renstrom, "Influence of confinement on the transition velocity of silicon carbide," *Proc. 23rd Int. Symp. Ballistics*, **2**, 1273-1280, Taragona, Spain (2007).

Appendix: X-Ray Data

The appendix contains the flash X-ray shadowgraphs and graphical representation of the data as measured in the X-rays. Table A-1 provides the times for the X-rays. Time zero is impact on the surface of the cover plate, which is located at -3.18 mm ("0" is the ceramic interface). Table A-2 lists the measured penetration depths and rod lengths at the corresponding X-ray times.

Table A-1. Raw X-ray Times (μs)

Exp./frame	1	2	3	4	5
11340	-8.177	6.990	21.870	36.881	51.866
11341	-9.388	5.817	20.626	35.618	50.699
11342	-6.957	5.068	13.004	18.129	29.087
11343	-9.596	2.572	10.436	15.368	26.464
11344	-4.844	3.326	10.208	17.274	23.279
11345	-6.057	2.129	8.912	15.934	21.982
11346	-5.086	4.043	9.919	16.970	21.976
11347	-4.701	2.436	7.247	12.290	17.314
11348	-5.358	2.809	9.689	16.881	22.739
11349	-12.769	12.260	27.161	42.206	57.145
11350	-13.451	11.655	26.602	41.682	56.626
11351	-13.072	12.003	26.925	42.124	56.989

Table A-2. Measurements from Flash X-Ray Shadowgraphs

	Pre-damaged (TS)				Intact (IT)		
	t after imp [μs]	pen depth [mm]	rod length [mm]		*t* after imp [μs]	pen depth [mm]	rod length [mm]
11341	50.70	34.37	30.77	**11340**	51.87	25.24	21.13
	35.62	21.90	41.25		36.88	15.43	33.32
	20.63	11.23	53.54		21.87	7.64	48.49
	5.82	1.17	65.90		6.99	0.43	63.66
	0.00	-3.18	70.07		0.00	-3.18	70.04
11343	26.46	30.10	46.93	**11342**	29.09	30.15	40.24
	15.37	15.92	56.33		18.13	16.30	50.12
	10.44	10.47	61.04		13.00	10.30	55.70
	2.57	0.82	68.52		5.07	2.74	65.03
	0.00	-3.18	70.01		0.00	-3.18	70.02
11345	21.98	26.64	48.33	**11344**	23.28	32.06	45.46
	15.93	18.64	54.12		17.27	22.91	51.80
	8.91	8.92	60.59		10.21	11.45	58.69
	2.13	0.06	68.41		3.33	1.68	66.43
	0.00	-3.18	70.02		0.00	-3.18	70.07
11346	21.98	29.61	46.70	**11347**	17.31	29.45	49.79
	16.97	21.99	51.92		12.29	19.43	55.14
	9.92	11.62	59.63		7.25	9.88	60.77
	4.04	2.99	66.17		2.44	1.49	67.59
	0.00	-3.18	69.98		0.00	-3.18	70.04
11349	57.14	15.24	17.40	**11348**	22.74	27.56	43.84
	42.21	13.26	33.43		16.88	19.17	49.96
	27.16	7.39	46.72		9.69	8.97	57.87
	12.26	3.33	61.61		2.81	1.22	67.41
	0.00	-3.18	70.06		0.00	-3.18	70.03
11351	56.99	27.68	28.47	**11350**	56.63	6.00	8.44
	42.12	19.92	39.00		41.68	4.58	25.26
	26.92	12.07	50.59		26.60	2.20	42.09
	12.00	3.63	61.34		11.65	1.03	59.95
	0.00	-3.18	70.12		0.00	-3.18	70.02

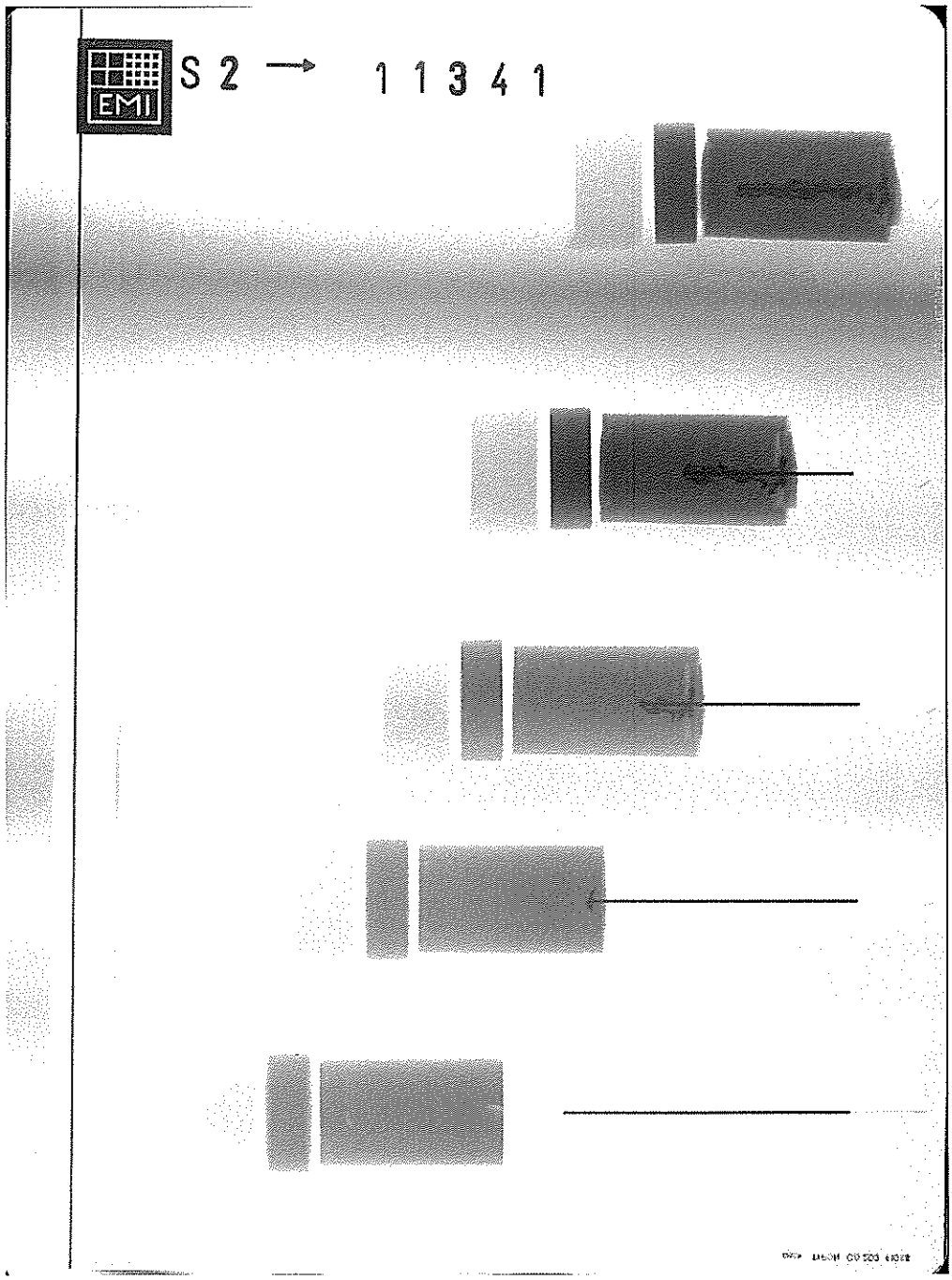

Figure A-1. X-ray picture for Exp. 11341: TS-SiC, v_p = 1.517 km/s.

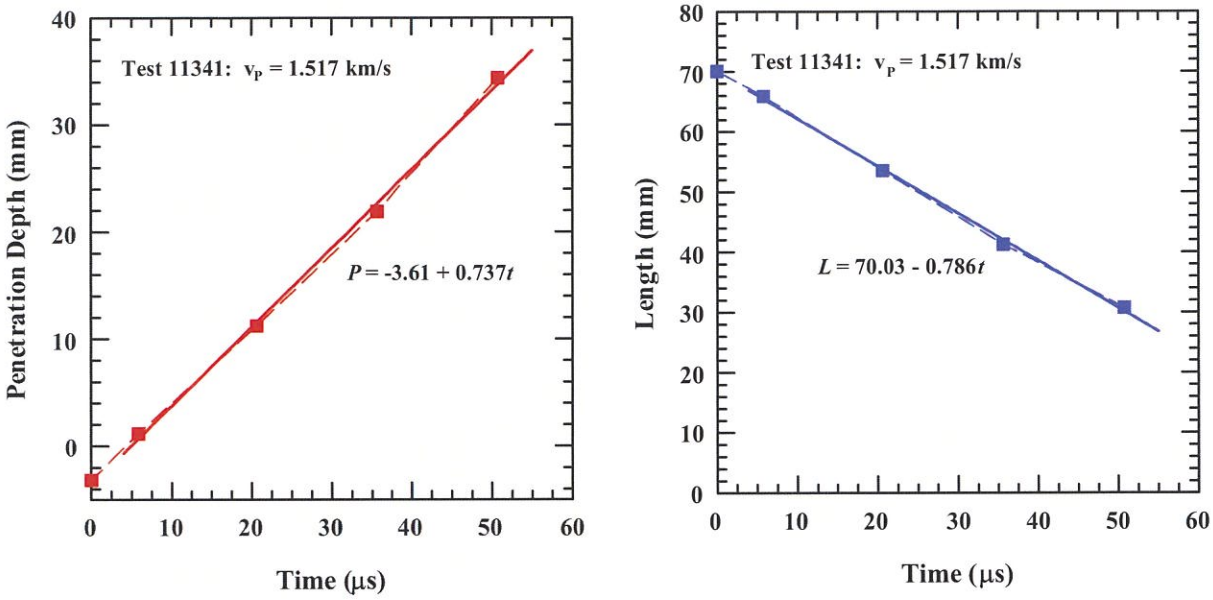

Figure A-2. Position-time and rod length versus time for Exp. 11341: TS-SiC.

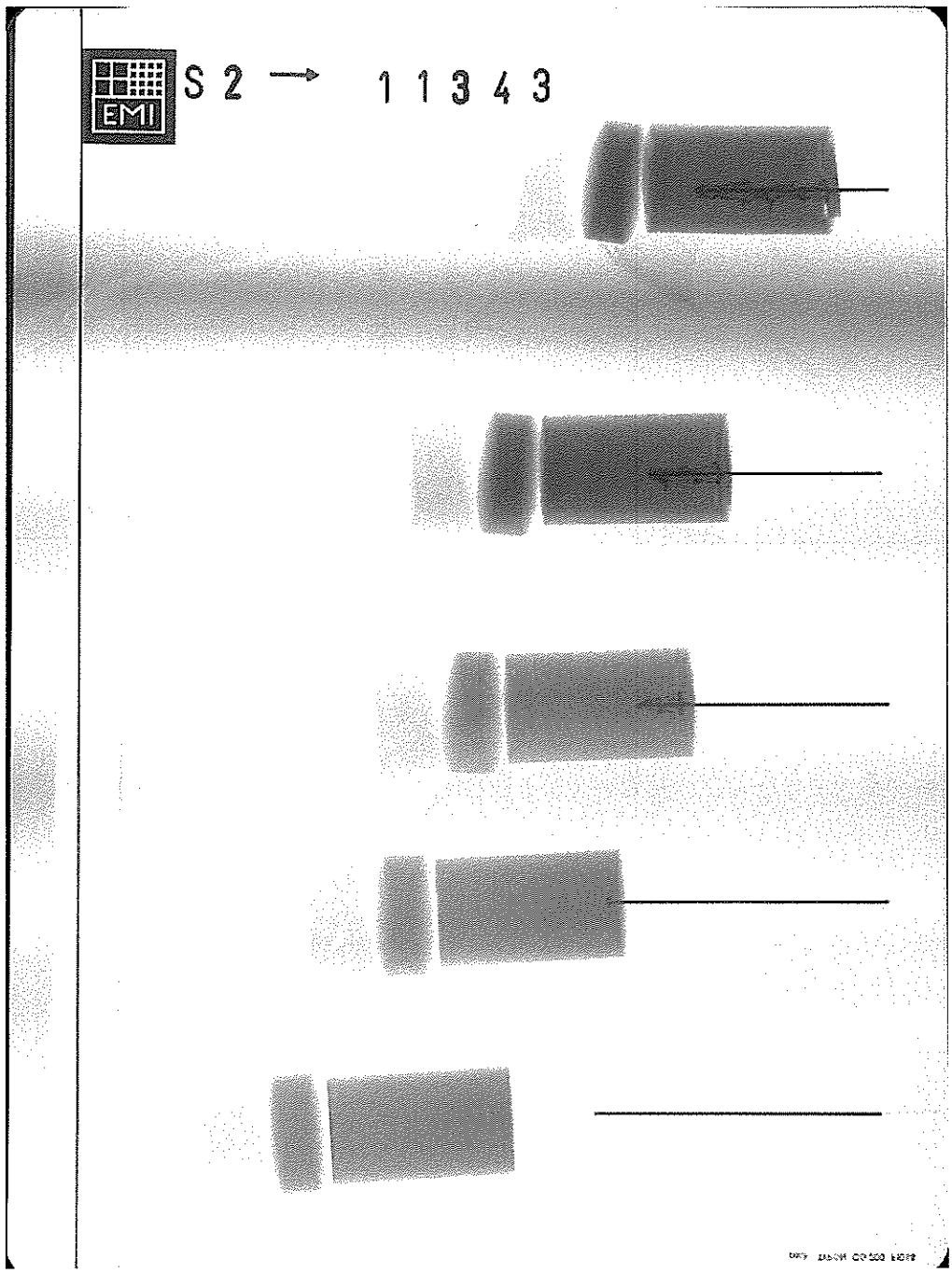

Figure A-3. X-ray picture for Exp. 11343: TS-SiC, v_p = 2.122 km/s.

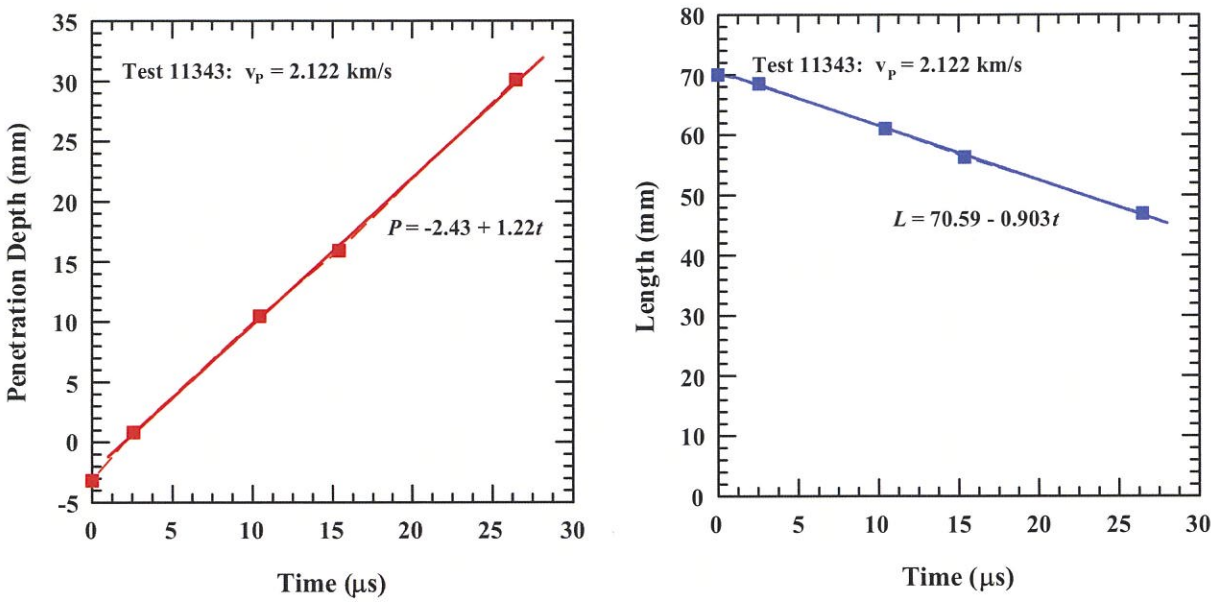

Figure A-4. Position-time and rod length versus time for Exp. 11343: TS-SiC.

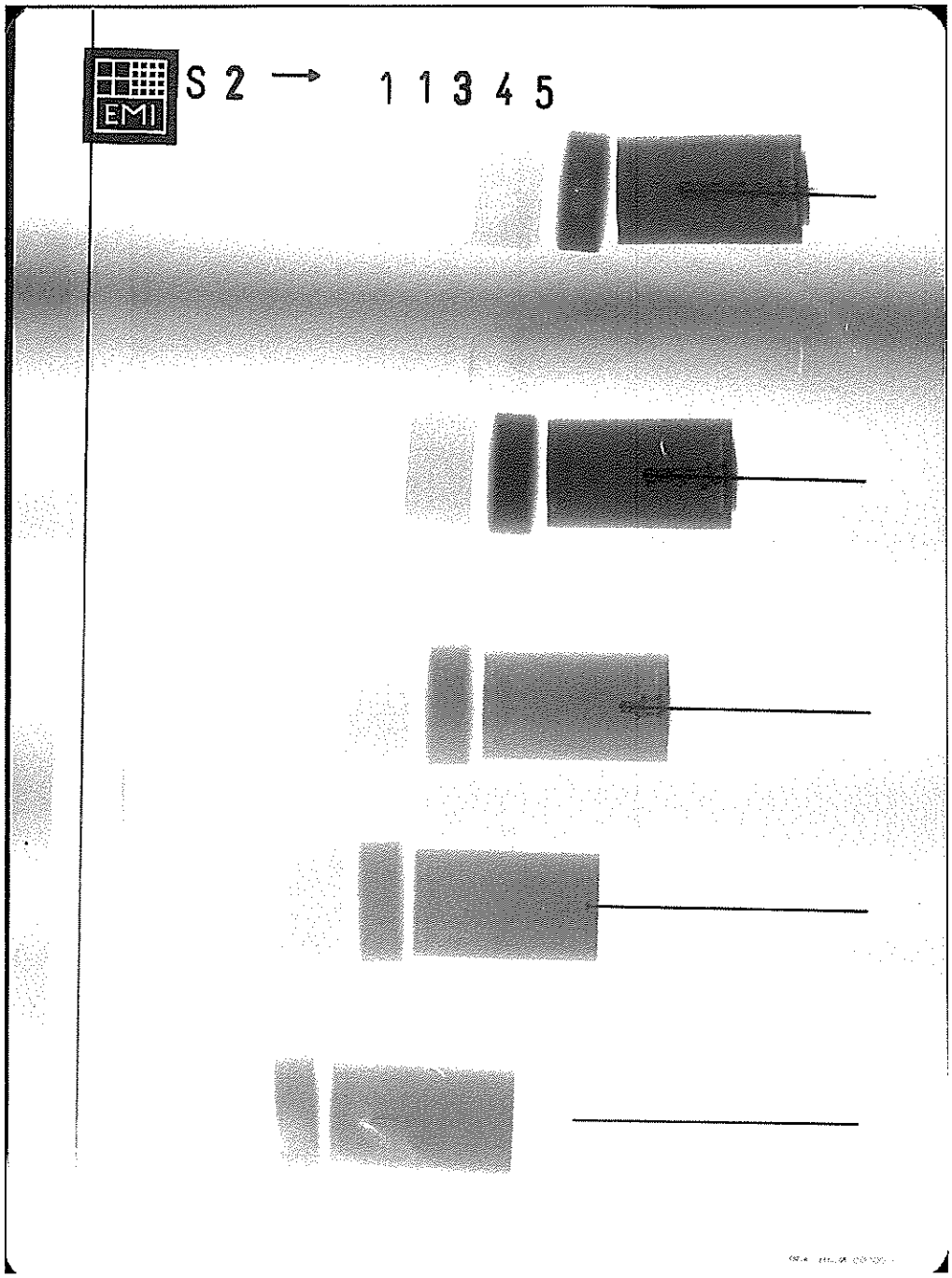

Figure A-5. X-ray picture for Exp. 11345: TS-SiC, v_p = 2.358 km/s.

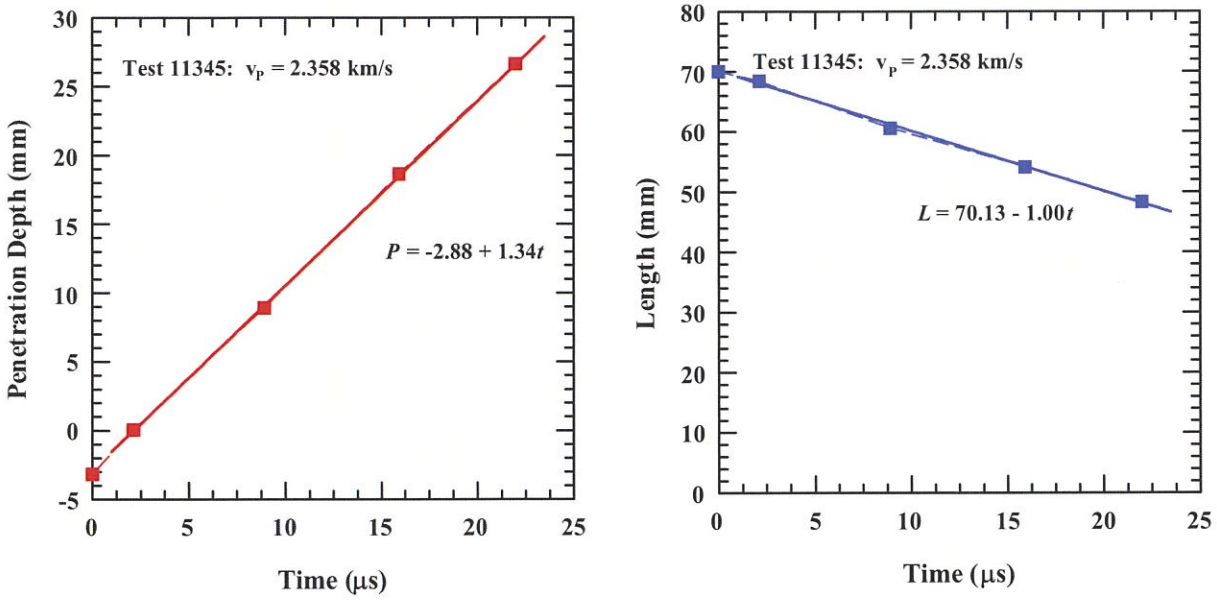

Figure A-6. Position-time and rod length versus time for Exp. 11345: TS-SiC.

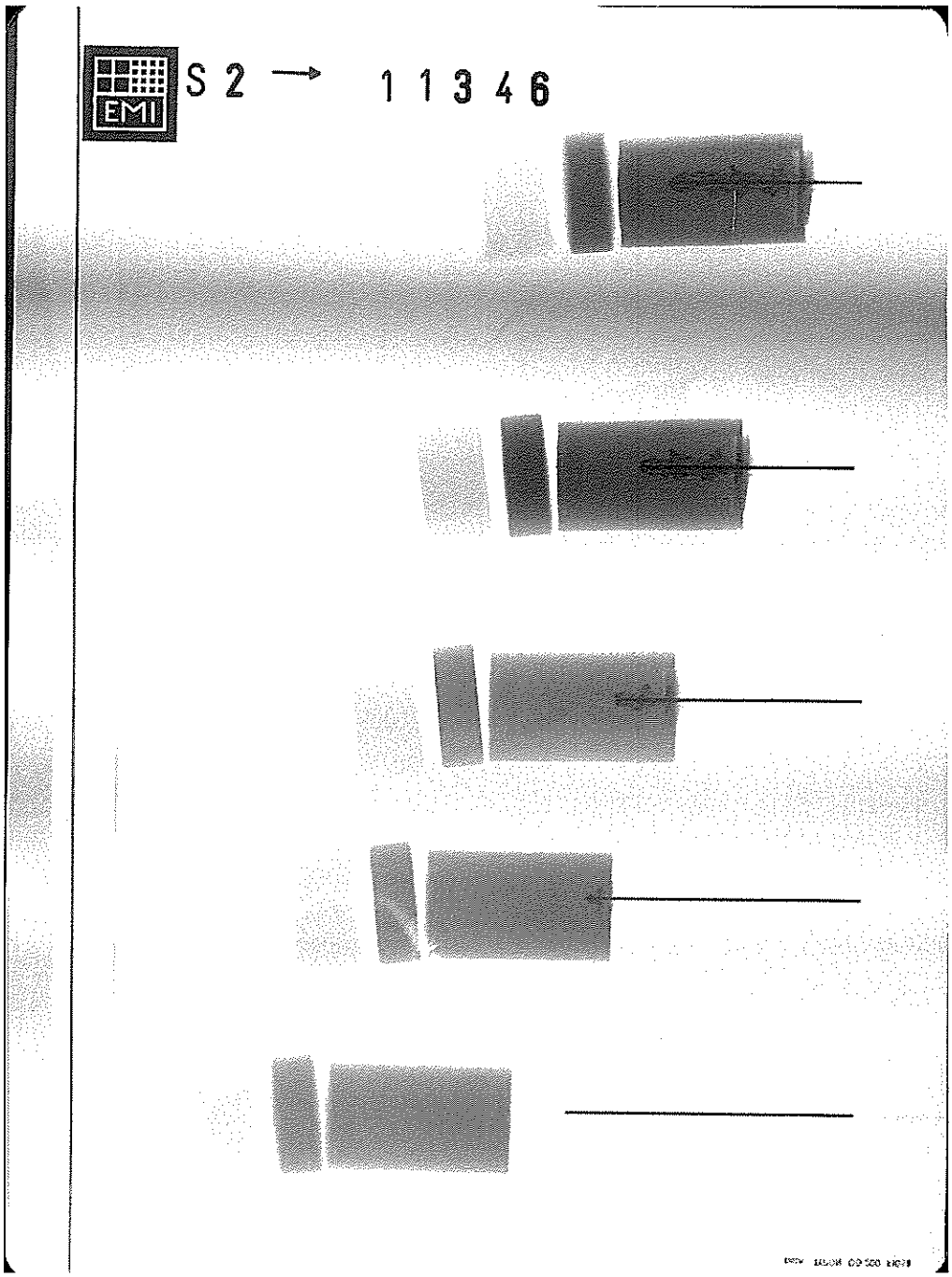

Figure A-7. X-ray picture for Exp. 11346: TS-SiC, v_p = 2.543 km/s.

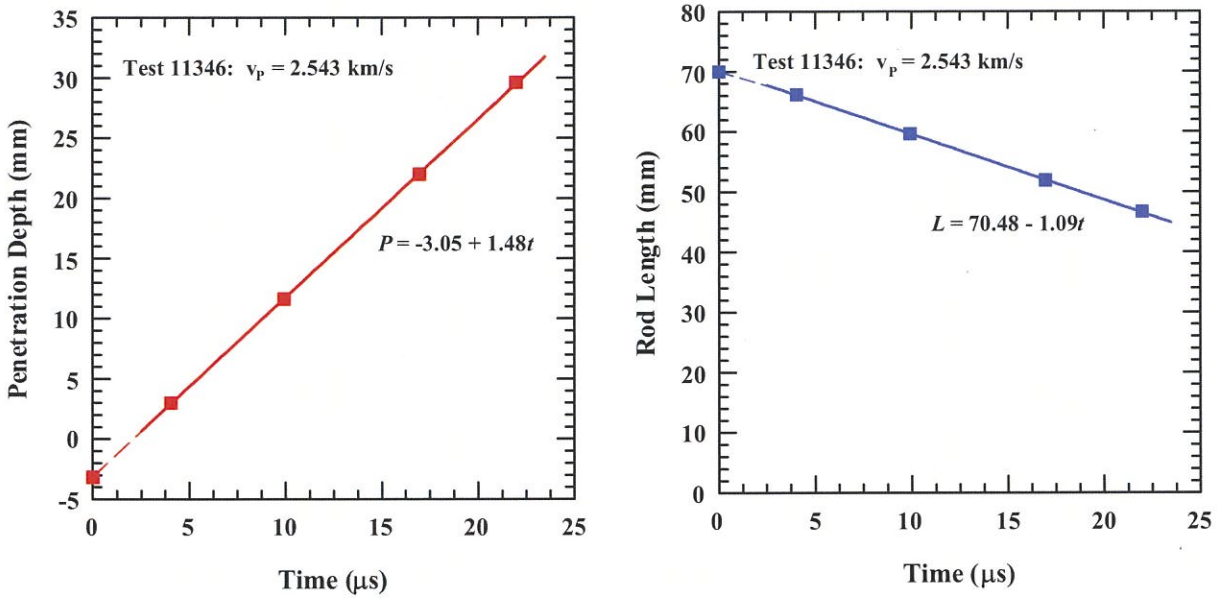

Figure A-8. Position-time and rod length versus time for Exp. 11346: TS-SiC.

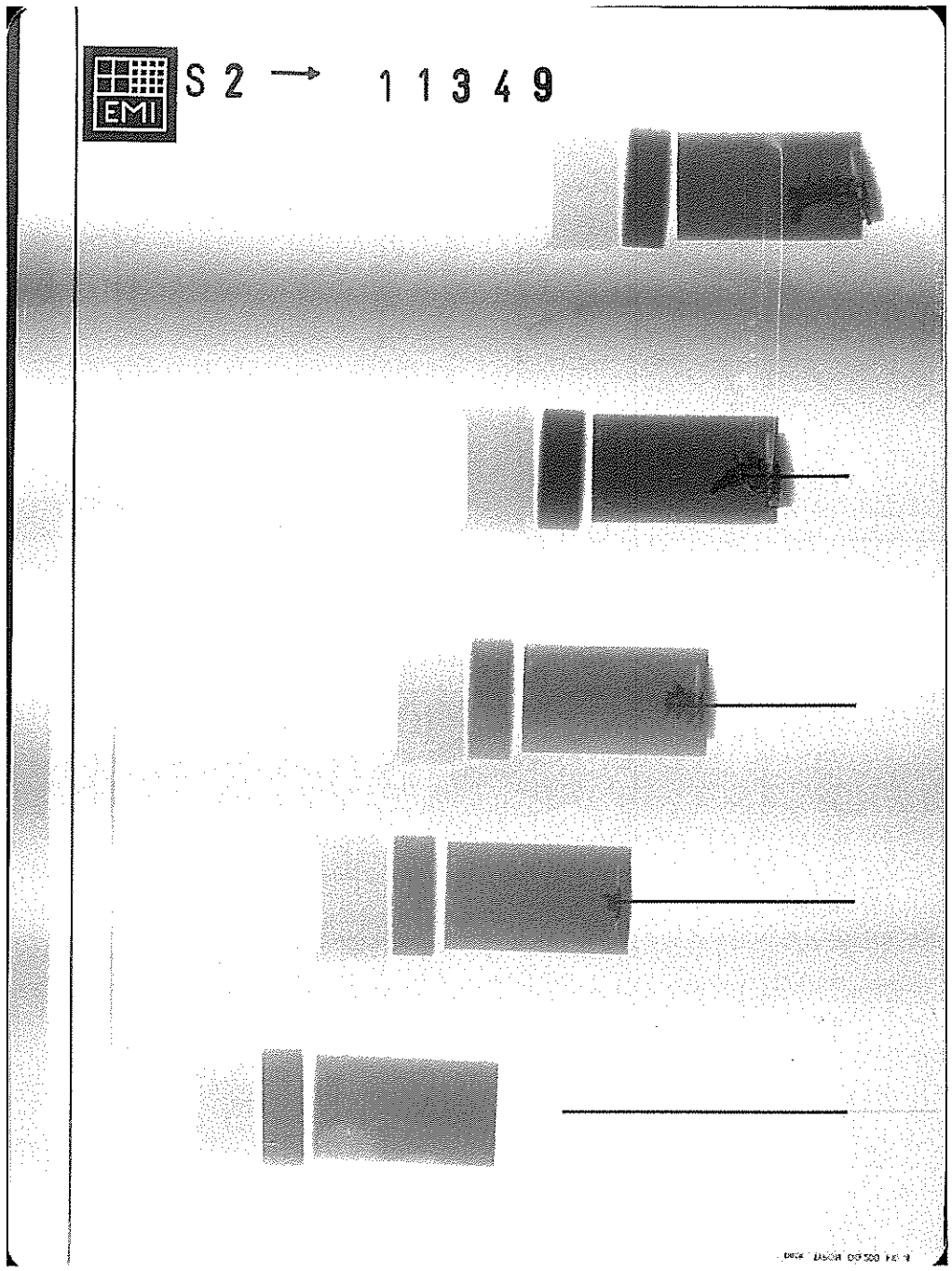

Figure A-9. X-ray picture for Exp. 11349: TS-SiC, v_p = 1.248 km/s.

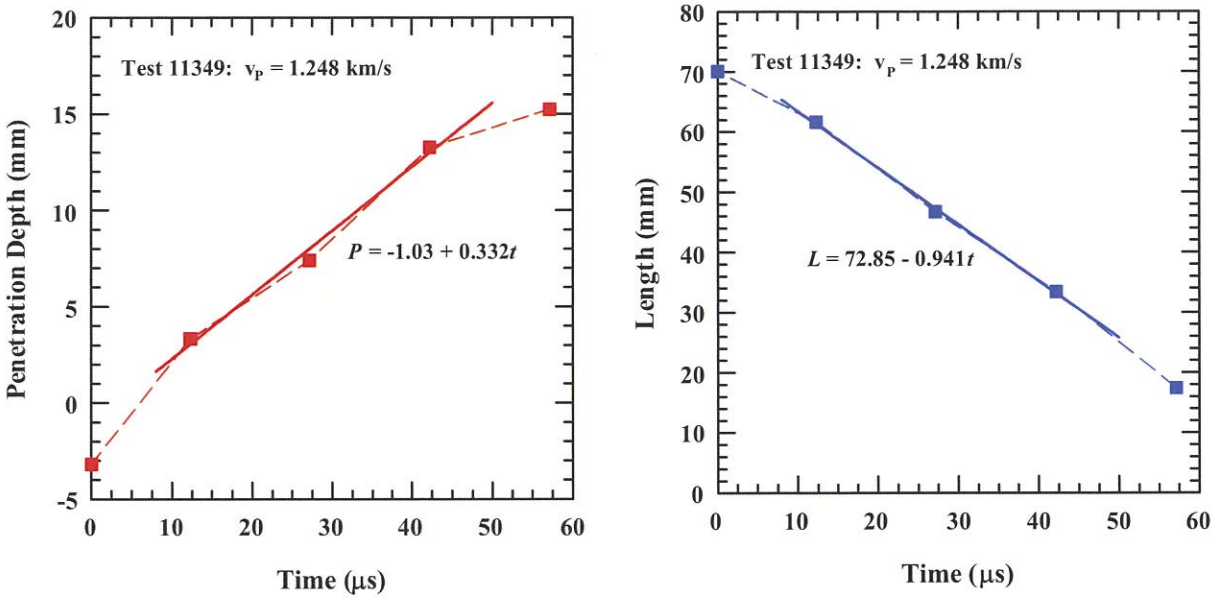

Figure A-10. Position-time and rod length versus time for Exp. 11349: TS-SiC.

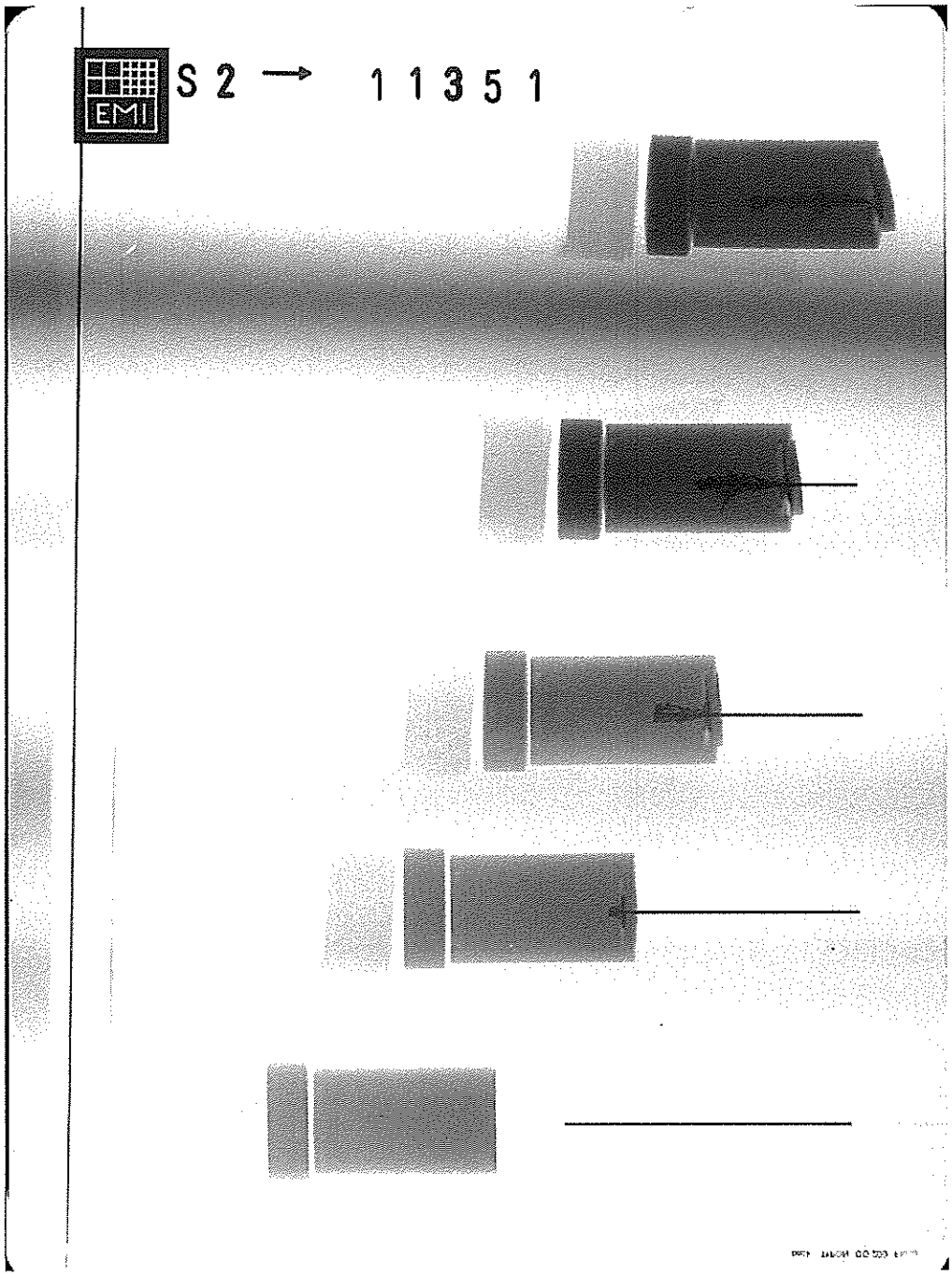

Figure A-11. X-ray picture for Exp. 11351: TS-SiC, v_p = 1.280 km/s.

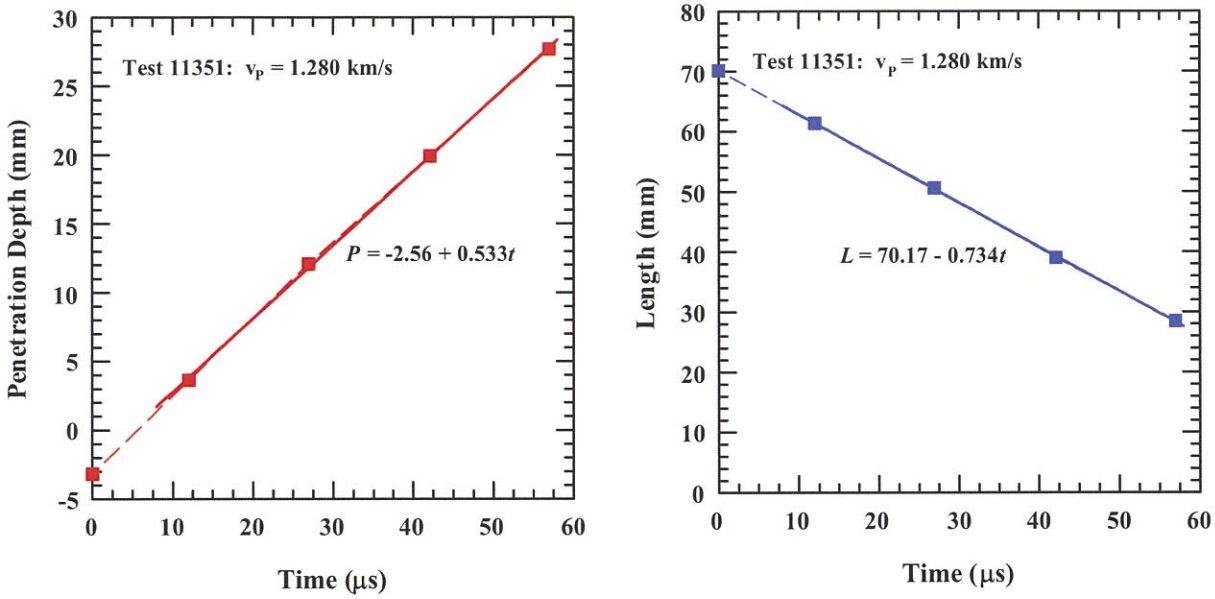

Figure A-12. Position-time and rod length versus time for Exp. 11351: TS-SiC.

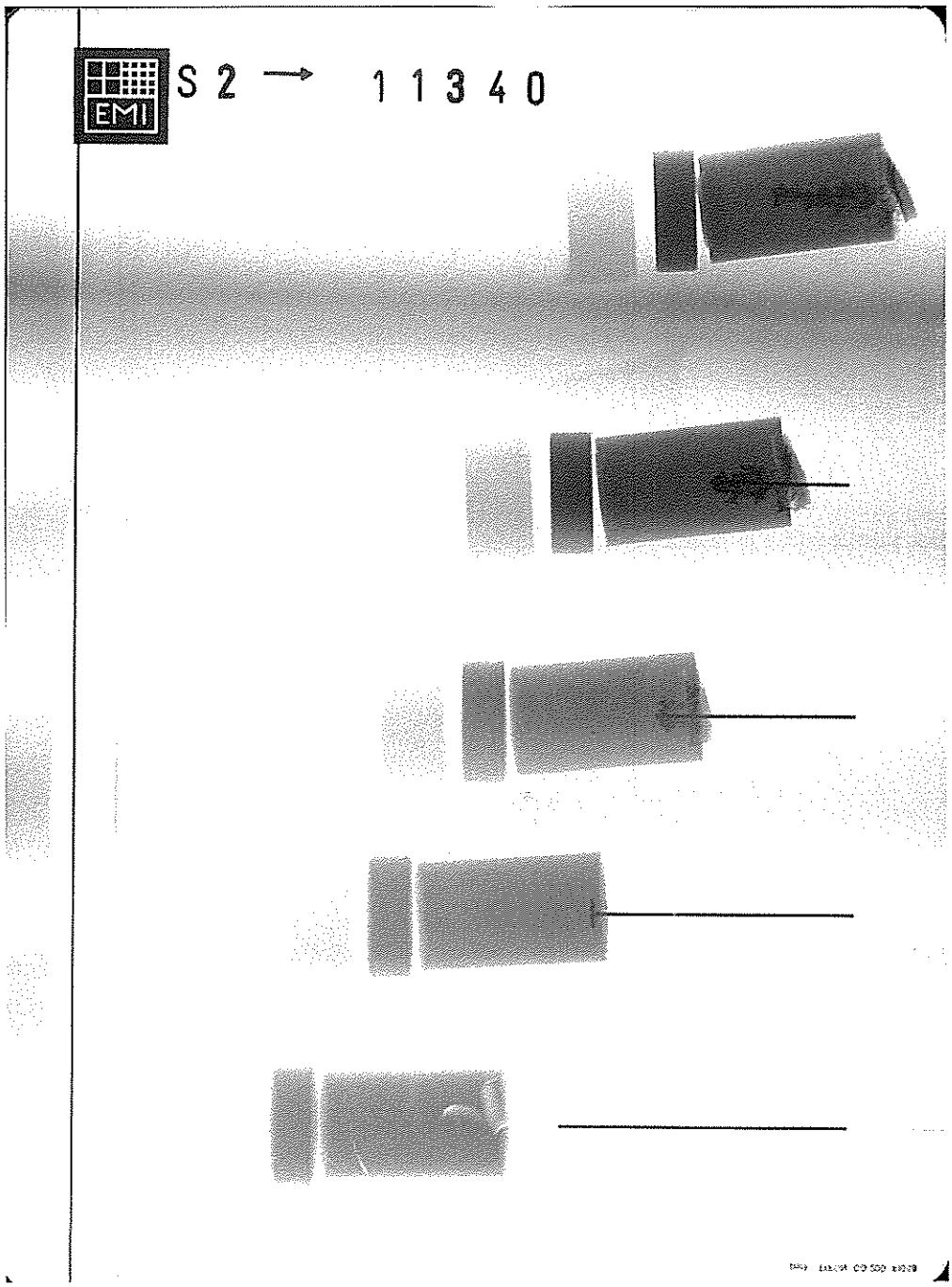

Figure A-13. X-ray picture for Exp. 11340: IT-SiC, v_p = 1.497 km/s.

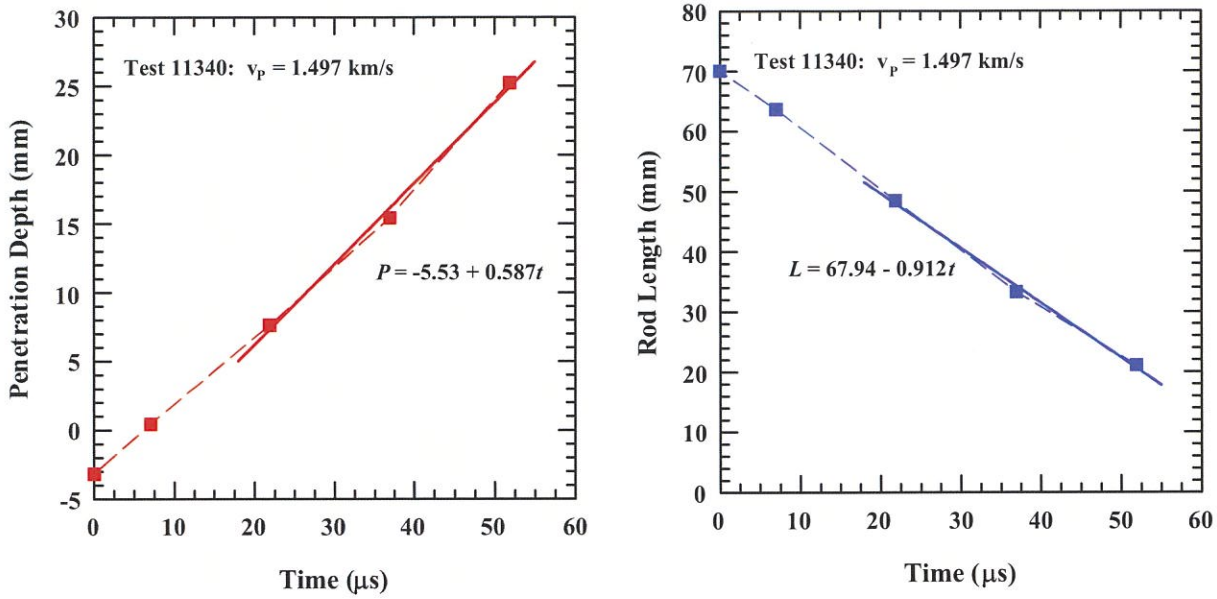

Figure A-14. Position-time and rod length versus time for Exp. 11340: IT-SiC.

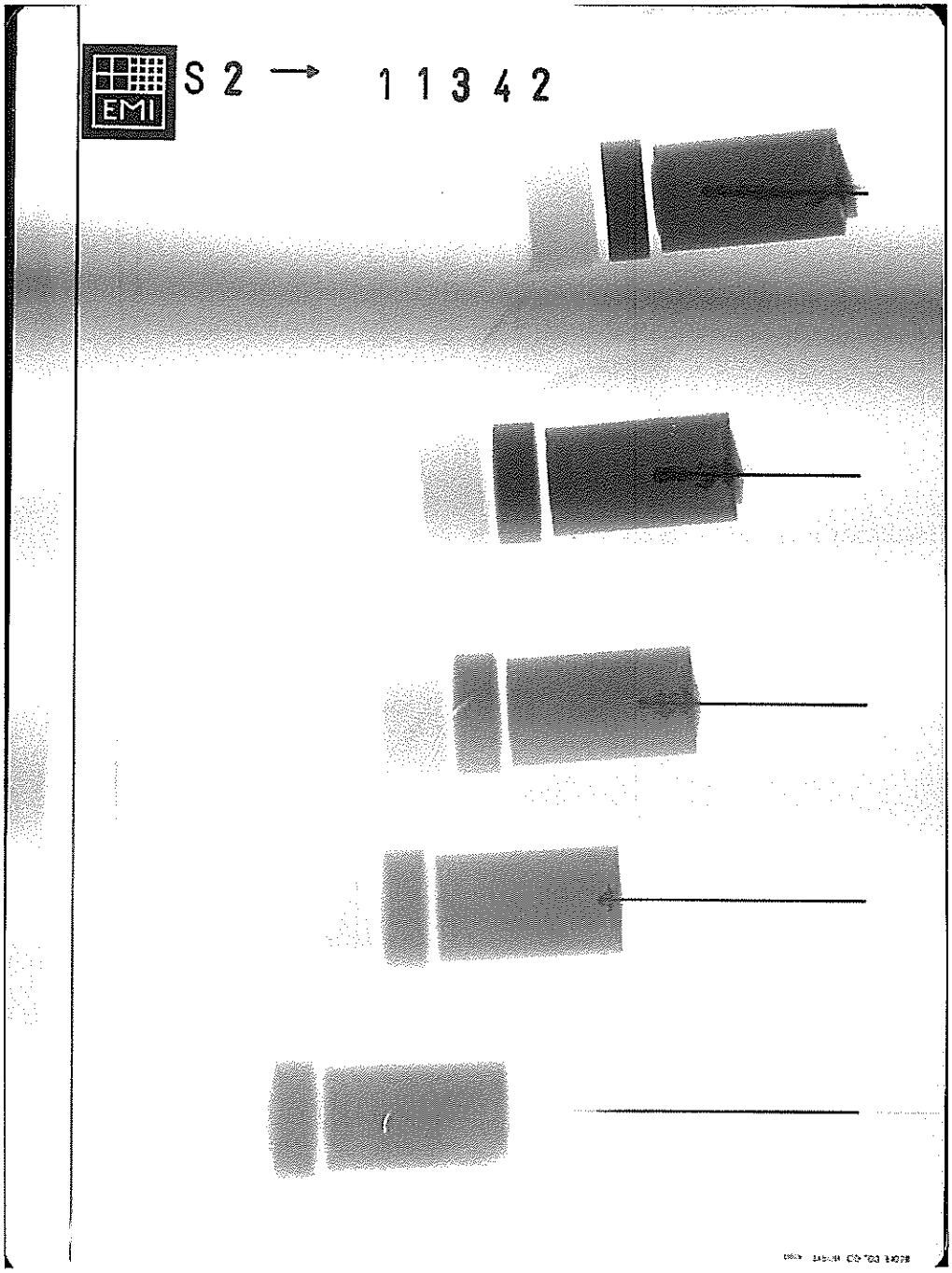

Figure A-15. X-ray picture for Exp. 11342: IT-SiC, v_p = 2.170 km/s.

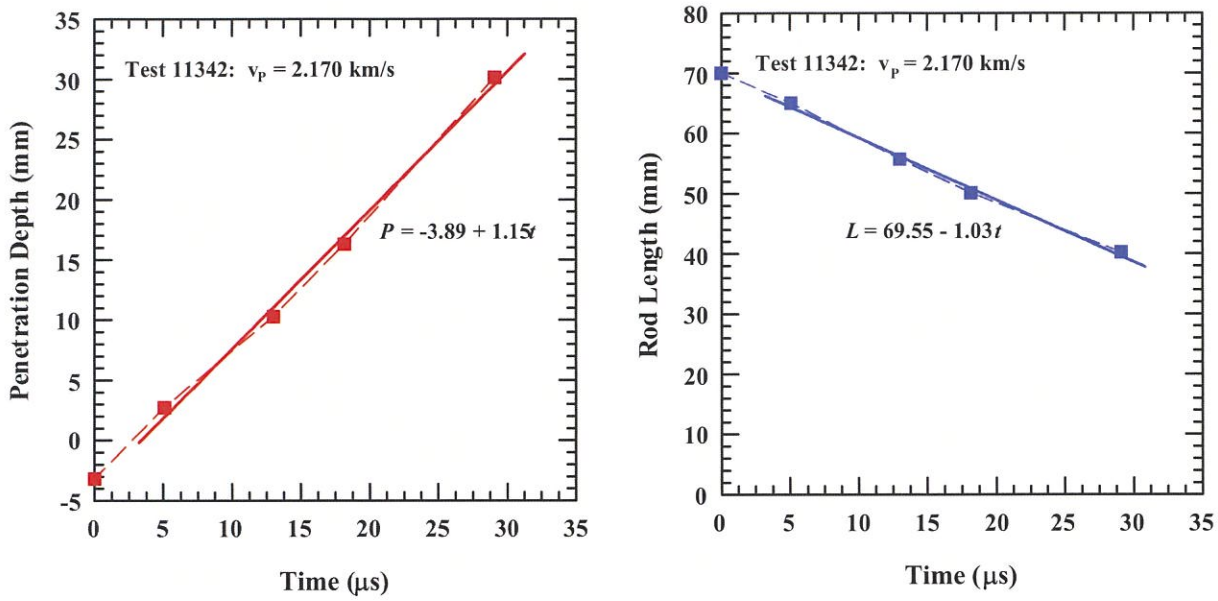

Figure A-16. Position-time and rod length versus time for Exp. 11342: IT-SiC.

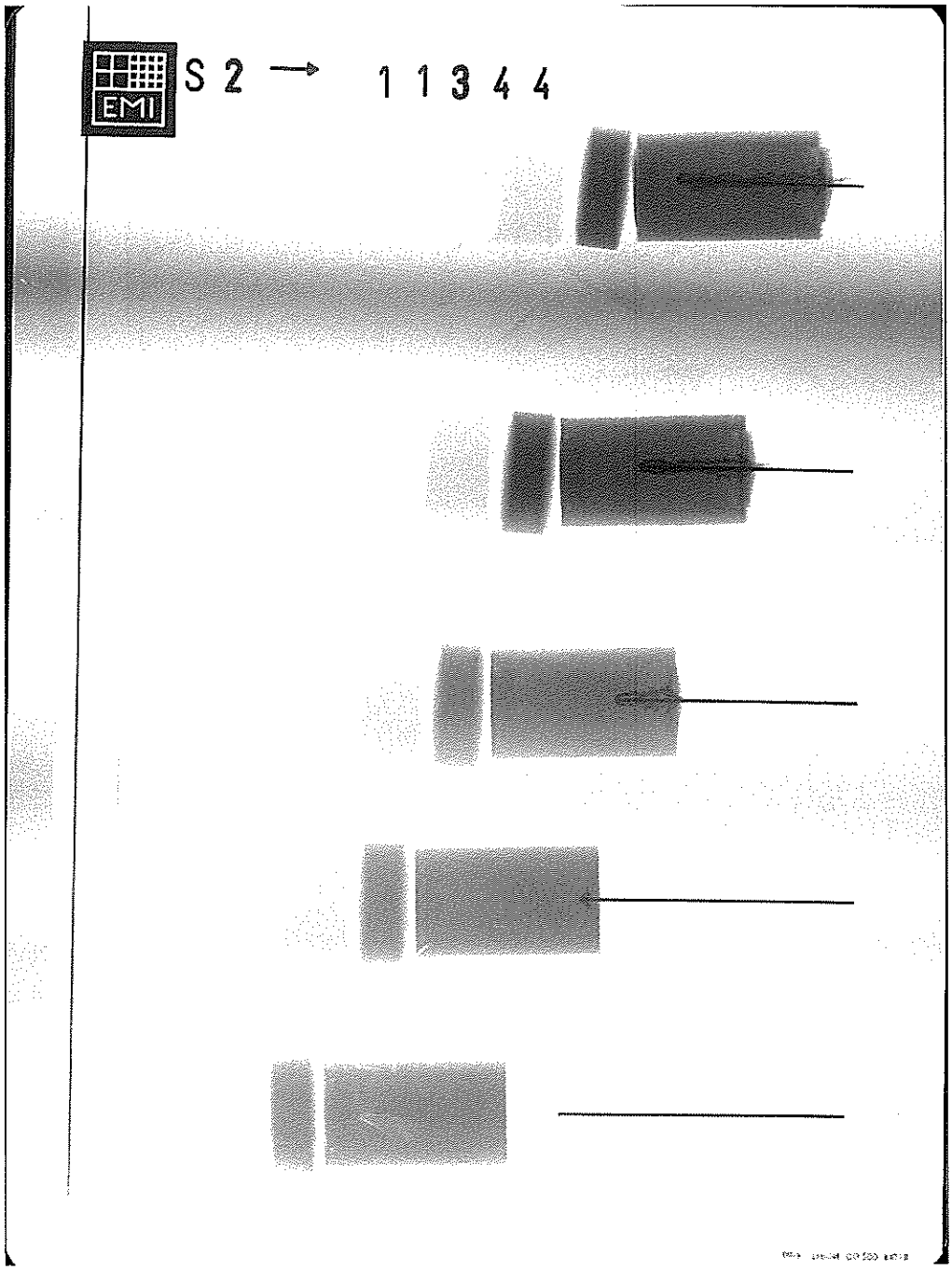

Figure A-17. X-ray picture for Exp. 11344: IT-SiC, v_p = 2.564 km/s.

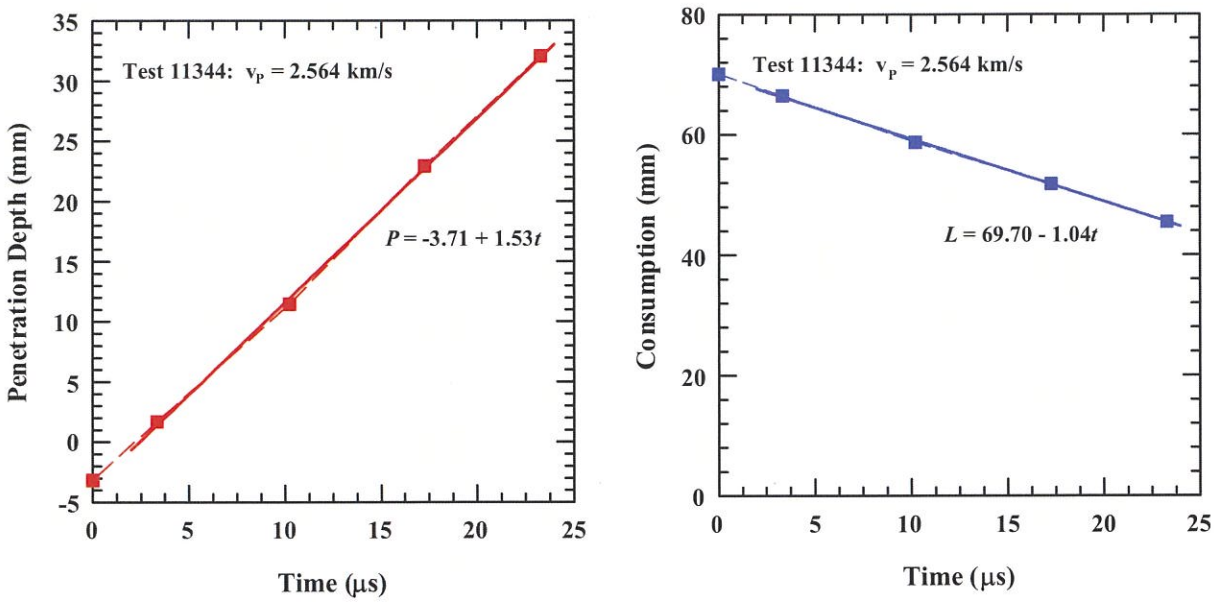

Figure A-18. Position-time and rod length versus time for Exp. 11344: IT-SiC.

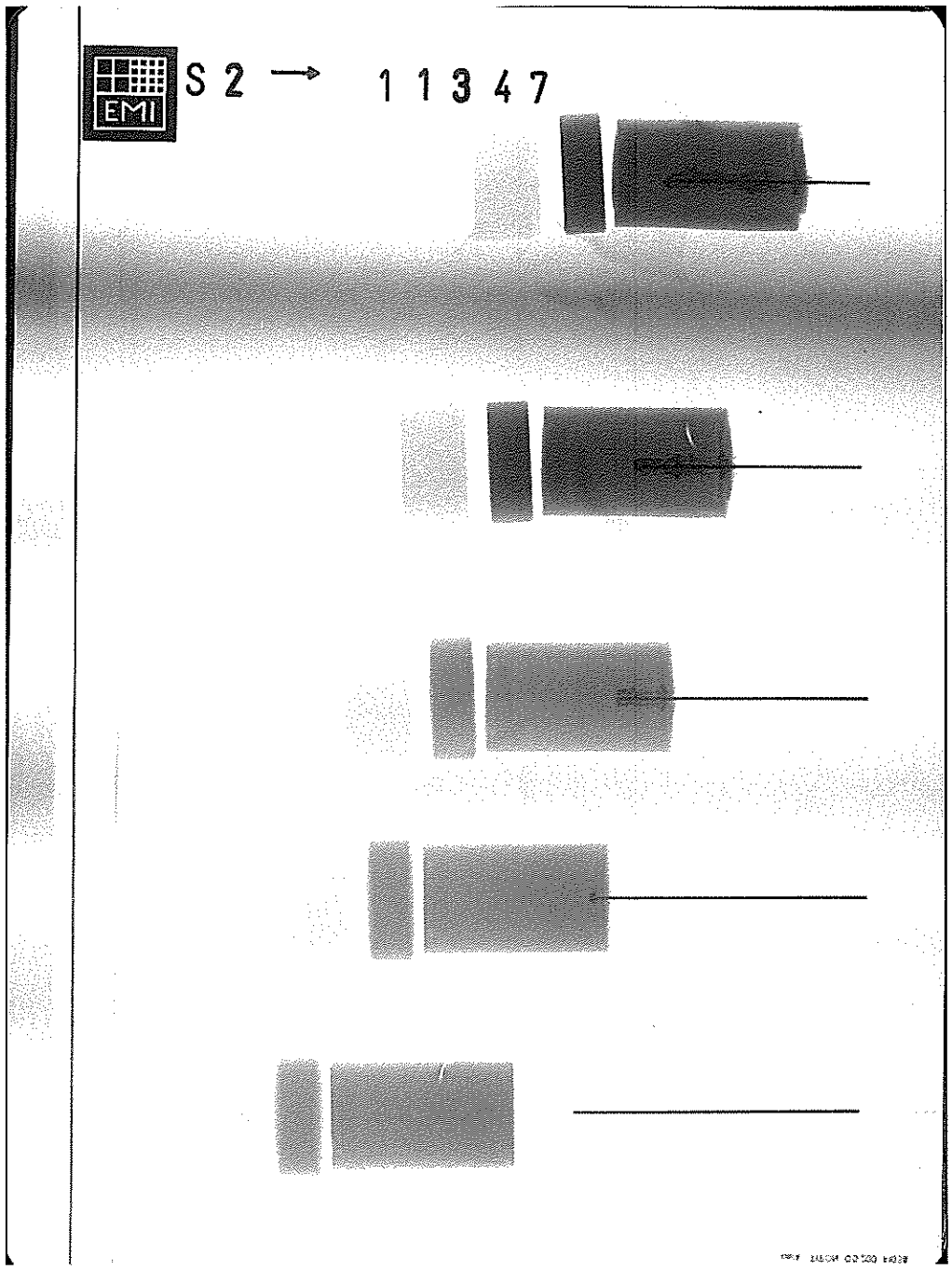

Figure A-19. X-ray picture for Exp. 11347: IT-SiC, v_p = 3.051 km/s.

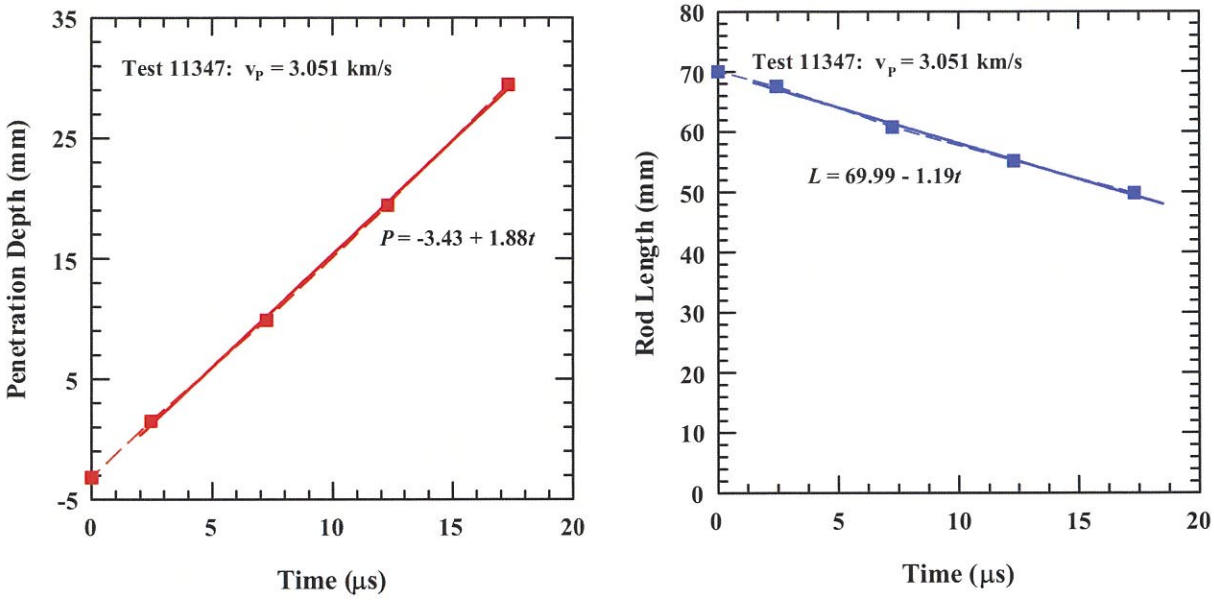

Figure A-20. Position-time and rod length versus time for Exp. 11347: IT-SiC.

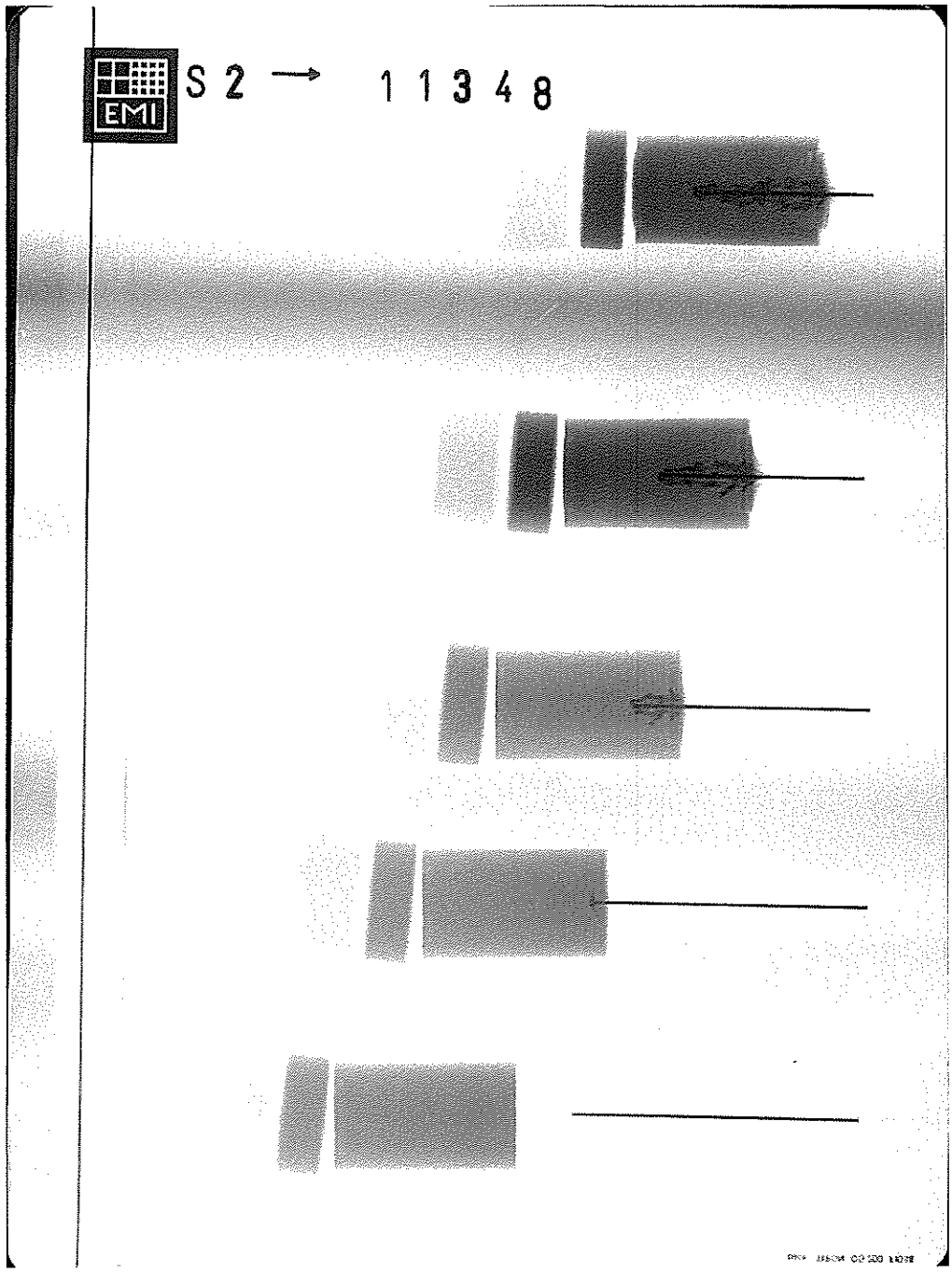

Figure A-21. X-ray picture for Exp. 11348: IT-SiC, v_p = 2.511 km/s.

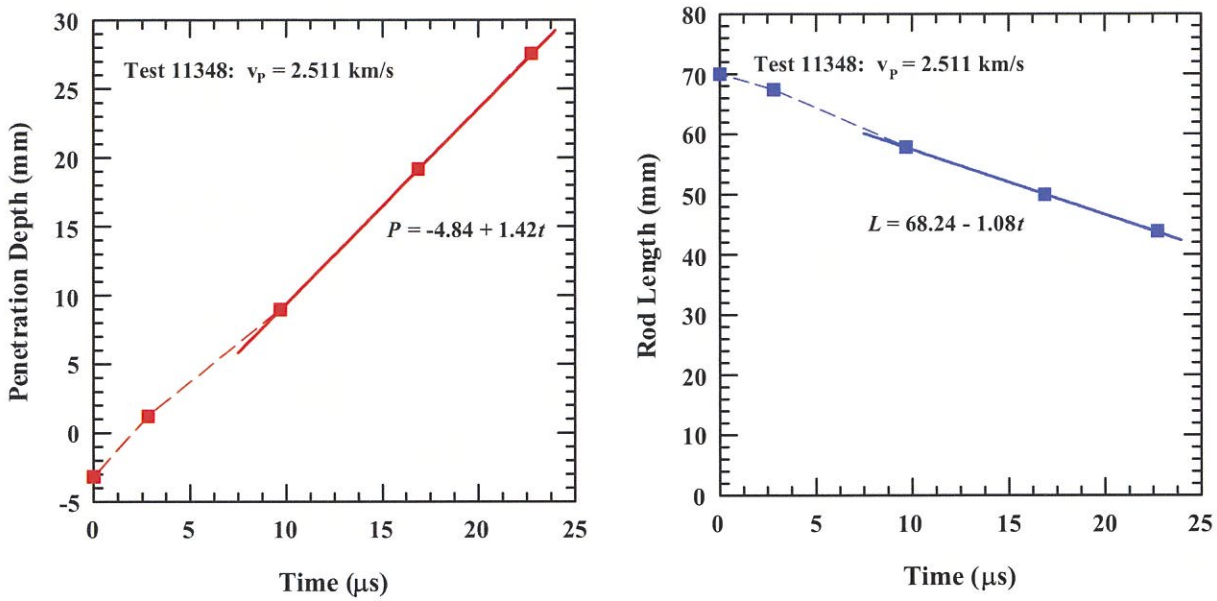

Figure A-22. Position-time and rod length versus time for Exp. 11348: IT-SiC.

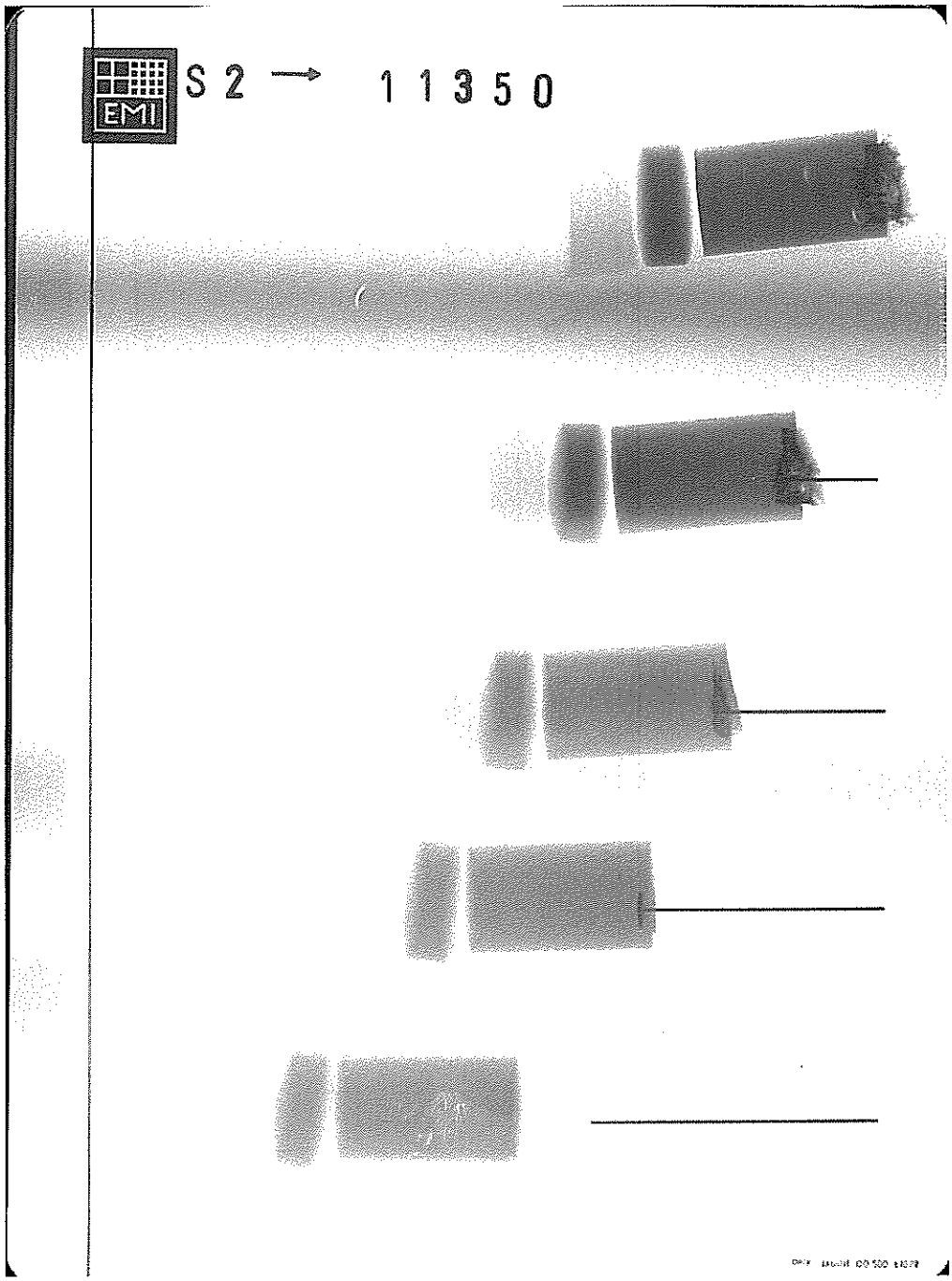

Figure A-23. X-ray picture for Exp. 11350: IT-SiC, v_p = 1.234 km/s.

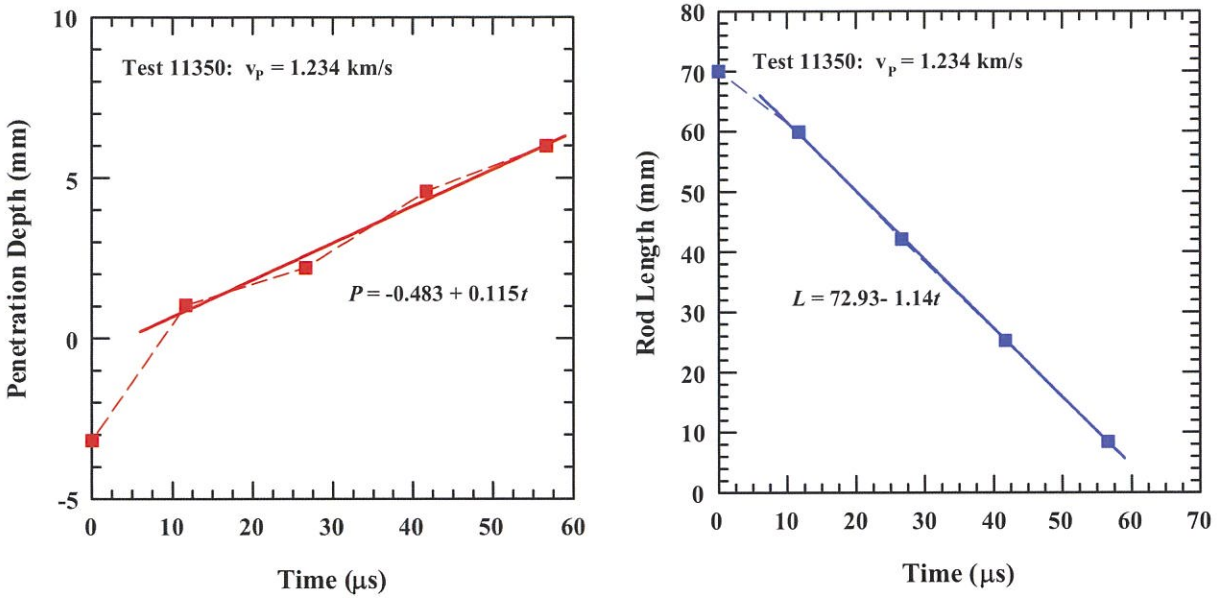

Figure A-24. Position-time and rod length versus time for Exp. 11350: IT-SiC.